



UNIVERSITÀ POLITECNICA DELLE MARCHE

FACOLTÀ DI INGEGNERIA

Master's degree in **Biomedical Engineering**

Development of a multi-parametric wearable device based on
electrocardiography and photoplethysmography.

Relatore:

Prof.ssa Burattini Laura

Tesi di Laurea di

Rollo Ilaria

Correlatore:

Cappelletti Mauro

A.A. 2020 / 2021

Abstract

The focus on wearable, non-invasive and portable devices is increasing, following the research and development of new solutions to provide biomedical signals with high accuracy and precision.

In particular, this work reports the design of a new device for home monitoring that combines electrocardiography (ECG) and Photoplethysmography (PPG) to obtain suitable parameters about the physiological state of humans.

The knowledge about the physiological event that will be monitored is always the starting point to design a new biomedical device. The section 'Physiological background' reassumes the anatomy and physiology of cardiocirculatory and respiratory system, that works in synergy to allow the functional activity of the human body.

The ECG signal mirrors the spreading of the contractile force of the heart cells through the body. It is generally collected as electrical signals that flow on the skin tissue.

The PPG signal is an optical technique that produces a signal able to follow up the cardiac cycle of the heart. This technique has a high spread in the pulse oximeter, a medical device typically used to measure blood oxygen saturation.

The developed prototype includes two sensors: a bioimpedance sensor and an optical sensor. The first one detects biopotential on the skin to obtain an ECG signal; the second is a multiwavelength sensor for PPG detection. Every sensor was tested on a developing board before producing the prototype of the device.

The preliminary test on the device concerned concerns the functionality of the sensors and its communication protocol.

The device collects raw data that are post analysed on MATLAB®. An algorithm filters the data and calculates the signal-to-noise ratio and the heart rate from the ECG recording of 6 healthy volunteers. The PPG results section includes the outcomes of a single green LED emitter tested on a healthy subject.

In the prototype, the PPG sensor is substituted with a multiwavelength sensor that permits the estimation of some physiological parameters, like oxygen saturation.

All the ECG recordings have a positive signal-to-noise ratio, and the waveform is confrontable with other certificate ECG devices.

The green LED has a high sensitivity that looks promise for further application and improvement of this multiparametric device.

In the future, this device could be implemented to be wear and used during daily activity and to follow up patients after their hospitalisation period.

Contents

Introduction	1
A. Physiological background	1
1 Cardiocirculatory system	1
1.1 Organs and Structures of the Cardiocirculatory System	1
1.2 Blood components	3
1.3 Electrical Activity of the Heart.....	6
1.4 Action Potential	7
1.5 Conduction system of the heart.....	10
1.6 Cardiac Cycle.....	12
1.7 Blood pressure.....	13
1.8 Arterial blood oxygen saturation	16
2 Physiology of Respiratory System.....	17
2.1 Organs and Structures of the Respiratory System	17
2.2 Mechanism of respiration: Ventilation	18
2.3 Mechanism of respiration: Gas Exchange	20
B. Physiological Signal analysis: origin and waveform description	22
3 Electrocardiographic signal description and acquisition	22
3.1 Origin of the signal	22
3.2 Signal acquisition.....	23
3.3 Signal description	26
4. Photoplethysmography: genesis and description of the signal.....	29
4.1 Origin of the Signal	29
4.2 Signal Acquisition	31
4.3 Signal description	33
4.3.1. Estimation of Arterial Oxygen Saturation.....	34
5. Heart Rate estimation from photoplethysmography and electrocardiography	36
C. State of the art of wearable sensors for daily monitoring	37
6. Wearable sensors for electrocardiogram	37

7. Wearable sensors for Photoplethysmographic signal	38
7.1 Sources of errors in Photoplethysmography recordings	39
7.2 Body location for Photoplethysmography sensors	40
D. Device development.....	41
8. Consideration behind the development of the device	41
9. Components of the device	43
10. Testing protocol of basic operations of the device	46
11. Testing protocol for sensors: background.	48
11.1 Experimental set-up for Electrocardiography	48
11.2 Experimental set-up for Photoplethysmography.....	50
12. Results.....	51
12.1 Electrocardiogram	51
12.2 Photoplethysmography	56
13. Discussion	59
Conclusion	II
Bibliography	III

Introduction

The focus on wearable, non-invasive and portable devices have a large spread nowadays. This focus has been driven mainly by increasing interest in home monitoring, which allows people to control their health by themselves.

With the ongoing research and development of new features capable of assessing and transmitting real-time biomedical data, the impact of wearables on medical diagnosis has become inevitable.

Thus, the development of new accurate medical devices and wearable sensors based on innovative technologies should grow.

Despite the potential of this new technology, as reported in scientific literature, the application of these devices in the field of health and clinical monitoring is still limited. While offering great potential, it is also important to evaluate ethical aspects related to the use of these smart devices without any expert supervision.

In the future, wearable devices may reduce hospitalization costs for weak people by monitoring their critical health conditions at home, thanks to their ability to provide a reliable clinical diagnosis by collecting physiological data over long periods.

In this scenario, the research and development of new solutions to provide biomedical signals with high accuracy and precision have significant importance.

As a matter of the fact, this work reports the preliminary phases of the design of a new device for home monitoring that combines electrocardiography (ECG) and Photoplethysmography (PPG) to obtain suitable parameters about the physiological state of humans.

A. Physiological background

1 Cardiocirculatory system

The cardiovascular system includes the heart, a muscular pump that drives the flow of blood; blood vessels, through which the blood flows; and blood, a fluid that circulates into the body, carrying materials to and from the cells. Its main role is the distribution of nutrients and hormones throughout the body, taking away waste products from tissues, and providing a mechanism for regulating temperature and consuming heat generated by the metabolic activities of the body's internal organs.

1.1 Organs and Structures of the Cardiocirculatory System

The heart is a muscular organ that generates a force that drives blood through the blood vessels.

The heart is divided by a central wall, the septum, into left and right halves. Each half comprises two chambers, an atrium and a ventricle, that are respectively the input and output of blood.

The right side moves deoxygenated blood that is loaded with carbon dioxide (CO₂) from the body to the lungs, and the left side receives oxygenated blood that has had most of its carbon dioxide removed from the lungs and pumps it to the body. The vessels that lead to and from the lungs make up the pulmonary circulation, and those that lead to and from the rest of the tissues in the body make up the systemic circulation (Figure 1).

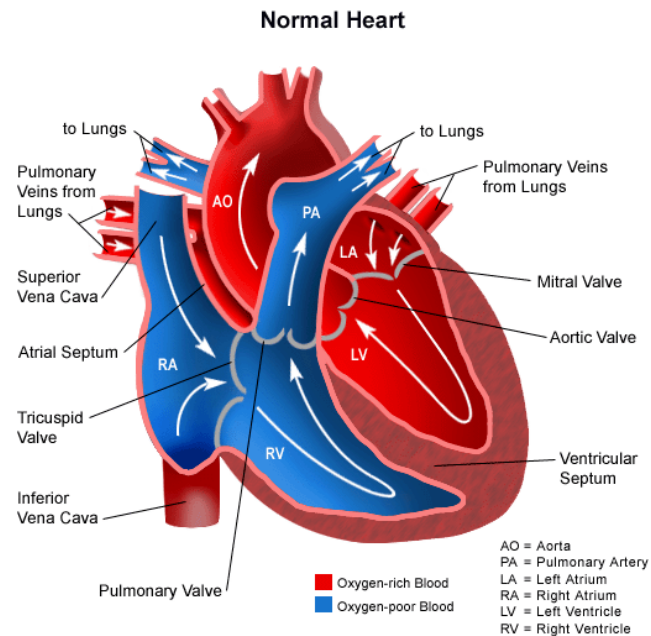


Figure 1: Main component of heart and blood flow inside the heart region.

Blood vessels that carry blood away from the heart are called arteries, while those that carry blood toward the heart are called veins. The smallest blood vessels are the capillaries, which are the site of exchange between blood and interstitial fluid. Proximity in the smallest blood vessels (capillaries) and living cells allows oxygen (O_2), carbon dioxide, and other small solutes to diffuse from the cells into the capillary and vice versa; the direction of diffusion depends on the concentration and partial pressure gradients inside cells and capillaries.

The heart wall consists of three layers: an outer layer of connective tissue called epicardium, a middle layer of cardiac muscle called myocardium, and an inner layer of epithelial cells called endothelium.

The rhythmic contraction and relaxation of the myocardium confer to the heart the pumping action.

When muscle in the wall of an atrium or ventricle contracts, the wall moves inward and push the blood into the chamber. This pushing increases the pressure within the chamber and forces the blood out. When the muscle relaxes, the chamber expands and fills with blood.

The cardiac cycle is the series of events that occurs in a heartbeat: the atria contract first, followed by the ventricles. This cycling causes variations of pressure in the chambers and changes the direction of pressure gradients for blood to flow. It is critical that blood flows through the heart in one direction. Thus, when the pressure gradients aid movement in the opposite direction, a series of valves avoids blood flow in this direction.

1.2 Blood components

Accounting for about 8% of total body weight, averaging 5,200 ml, blood is a heterogeneous suspension of elements (the blood cells, or hematocytes) suspended in a continuous, straw-coloured fluid called plasma. Adult males typically average about 5 to 6 litres of blood. Females average 4–5 litres.

Blood has a viscosity approximately five times greater than water. Viscosity is a measure of a fluid's thickness or resistance to flow and hangs on the presence of the plasma proteins and formed elements within the blood. The viscosity of blood has a significant impact on blood pressure and flow.

The more viscous fluids would demonstrate higher resistance to flow than the less viscous ones.

The hematocytes include three basic types of cells: red blood cells (erythrocytes, 95% of the corpuscles elements), white blood cells (leukocytes, averaging less than 15% of all hematocytes), and platelets (thrombocytes, on the order of 5% of all blood cells).

The erythrocytes are the most abundant formed elements: a single drop of blood contains millions of erythrocytes and just thousands of leukocytes. They are quite small cells, with a mean diameter of only about 7–8 μm . The primary functions of erythrocytes are to carry on inhaled oxygen from the lungs and transport it to the body's tissues, and to carry out carbon dioxide waste at the tissues and transport it to the lungs for exhalation. Erythrocytes remain within the vascular network.

The primary function of leukocytes is to identify and dispose of foreign substances (such as infectious organisms) that do not belong to the human body. One of the most distinctive characteristics of leukocytes is their movement. Whereas erythrocytes never leave the blood network, leukocytes routinely leave the bloodstream to perform their defensive functions in the body's tissues: the vascular network is simply a highway to travel and soon exit to reach their destination.

Platelets participate in the blood clotting process. Platelets are relatively small, 2–4 μm in diameter, but numerous. After coming into circulation, approximately one-third migrate to the spleen for storage for later diffusion in response to any rupture in a blood vessel. Then they become activate to perform their primary function, which is to limit bleeding. Platelets remain only about 10 days then they are phagocytized by macrophages.

Platelets are critical to haemostasis, the stoppage of blood flow following damage to a vessel. They also secrete some growth factors essential for growth and repair of tissue, particularly connective tissue.

Like other fluids in the body, plasma is composed primarily of water, about 92%. Dissolved or suspended within water is a mixture of substances, most of

which are proteins. There are hundreds of substances dissolved or suspended in the plasma, although many of them are found only in small quantities.

A fundamental role for gas exchange is solved by Haemoglobin (Hb), that is a two-way respiratory carrier, transporting oxygen from the lungs to the tissues and facilitating the return transport of carbon dioxide.

Haemoglobin is a large molecule composed of proteins and iron (Figure 2). Each Hb molecule contains four heme groups surrounding a globin group, forming a tetrahedral structure. Heme, which accounts for only 4% of the entire weight of the molecule, is composed of a ringlike organic compound known as a porphyrin to which an iron atom is attached.

Iron atom binds oxygen as the blood travels between the lungs and the tissues. There are four iron atoms in each molecule of haemoglobin, which accordingly can bind four molecules of oxygen. Globin consists of two linked pairs of polypeptide chains.

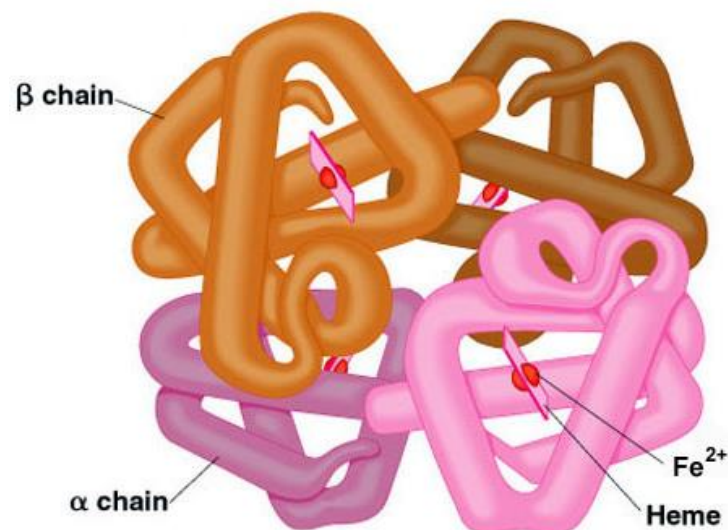


Figure 2: Structure of haemoglobin.

In the arterial circulation, haemoglobin has a high affinity for oxygen and a low affinity for carbon dioxide, organic phosphates, and hydrogen and chloride ions. In the venous circulation, these relative affinities are reversed.

As a matter of fact, in the lungs, haemoglobin carries on oxygen, which binds to the iron ions, forming oxyhaemoglobin. The bright red, oxygenated haemoglobin (HbO₂) travels to the body tissues, where it releases some of the oxygen molecules, becoming darker red deoxyhaemoglobin, sometimes referred to as reduced haemoglobin.

Oxygen release depends on the demand for oxygen in the surrounding tissues, so haemoglobin rarely departs all its oxygen behind. In the capillaries, CO₂ enters the bloodstream. About 76% dissolves in the plasma, some of it remaining as dissolved CO₂, and the remainder forming bicarbonate ion.

As mentioned previously, the primary function of Hb is to transport O₂ from the lung to tissues, binding and releasing O₂.

1.3 Electrical Activity of the Heart

The cardiac muscle, unlike skeletal muscle, does not require inputs from the central nervous system to contract. Instead, cardiac muscle contractions are triggered by signals originating from within the muscle itself. The ability of the heart to generate its rhythm is called auto rhythmicity.

A particular kind of cell, called autorhythmic cell, is responsible for the spontaneous activity of the heart. They involve two main groups with different functions: pacemaker cells, which initiate action potentials and determine the heart rhythm, and conduction fibres, which transmit action potentials through the heart in a highly coordinated manner. Collectively, these cells bring up the

conduction system of the heart. The cells that generate the contractile force are called contractile cells.

Pacemaker cells are concentrated primarily in two specific regions of the myocardium: the sinoatrial node (SA node), located in the wall of the upper right atrium near where it joins with the superior vena cava, and the atrioventricular node (AV node), located near the tricuspid valve in the interatrial septum. SA node is the actual pacemaker of the heart. Pacemaker cells in the SA node have a faster inherent rate of spontaneous depolarization, and the SA node and AV node are connected, the SA node drives the depolarization of the cells in the AV node and throughout the heart, thereby establishing the heart rate.

1.4 Action Potential

An electrical impulse due to variations in membrane potential is the reason for myocardial contraction and relaxation in a cardiac cycle.

This electrical impulse is a consequence of rapid changes in the membrane potential, named action potential (Figure 3). The genesis of the action potential is due to variations of ions concentration inside and outside the cell membrane.

As a matter of fact, ions, mainly sodium (Na^+), potassium (K^+), and calcium (Ca^{2+}), are present in different concentrations inside the cells and their surrounding environments. Sodium and calcium concentrations are higher in extracellular fluid, while potassium is present at a higher concentration inside the cell. Voltage-sensitive ion channels are available on cellular membranes to facilitate the movement of these ions. The tendency of ions to move down their chemical gradient and the inclination for charges to balance out across membranes contributes to a net electrochemical potential that varies with the status of ion channels.

In resting conditions, the membrane potential of -70 mV is measured and it is called resting potential.

During an action potential a consistent, rapid depolarization occurs: the polarity of the membrane potential reverses so, the membrane potential becomes positive for a brief time. The membrane potential changes very quickly (in about 1 msec) from a resting level of approximately -70 mV to +30 mV (a change of 100 mV).

Once initiated, an action potential is capable of being propagated long distances without any decrease in strength.

The threshold potential is different for conductive cells and pacemaker cells (-40 mV). Cells can reach threshold potential through stimulus by either adjacent cells, or, if they are pacemaker cells, possess automaticity.

Once an action potential is initiated in pacemaker cells, rapid transmission of action potentials from pacemakers to conduction fibres to the contractile cells is possible because all cardiac muscle cells are connected to their neighbours by gap junctions, which permit electrical current to pass in the form of ions from one cell to another, and by desmosomes, that are the mechanical junction between adjacent cells.

Generally, action potential has five distinct phases. Instead, a pacemaker action potential has only three phases, designated phases zero, three, and four.

Phase zero is the phase of depolarization. The voltage-gated Ca^{2+} channels open as soon as they reach the threshold, causing the influx of Ca^{2+} ions. This influx of cation results in an upstroke in membrane potential from -40 mV to +10 mV. Because calcium channels are slow channels (compared to sodium channels), the upstroke is not as steep as that of cardiomyocytes.

Phase three is repolarization, involving the closing of Ca^{2+} channels, blocking the flow of Ca^{2+} ions. Voltage-gated K^{+} channels open, allowing for efflux of K^{+}

ions. This efflux of cation contributes to a rapid decrease of membrane potential from +10 mV to -60 mV.

Phase four, a phase of gradual depolarization, is unique to the pacemaker cells. This gradual depolarization mainly occurs via a depolarization current or pacemaker current, due to the slow influx of Na^+ ions. This pacemaker current causes the membrane potential to change from -60 mV to reach the threshold potential of -40 mV. The slope of phase four determines heart rate and is different for pacemaker cells in different regions. SA node pacemaker cells depolarize at a rate of 60 to 100 per minute, while the AV node at 40 to 60 per minute.

The cardiac myocyte action potential is different from that of pacemaker cells and has five phases, zero through four.

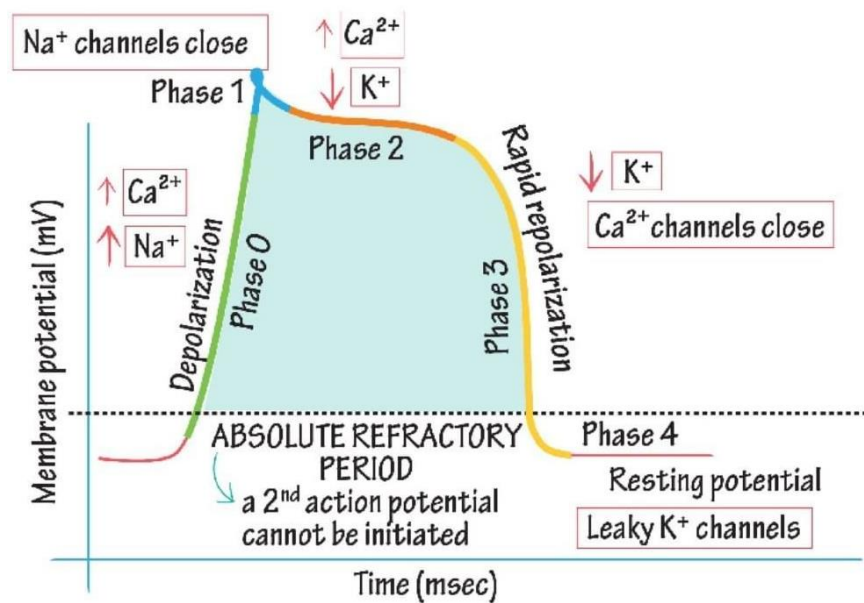


Figure 3: Cardiac Action Potential waveform and its phases in relationship of chemical phenomena that occurs across cell membrane.

During phase zero, the phase of rapid depolarization the membrane potential changes from -70 mV to +50 mV. The voltage-gated sodium channels are faster channels than calcium channels, and hence we get a steep upstroke of the action potential.

In phase one, there is inactivation of the previously opened voltage-gated Na⁺ channels along with the activation of transient outward potassium current. A slight decline in the membrane electrochemical potential results at the beginning of phase two.

During phase two or Plateau phase, Ca²⁺ influx occurs and balances the K⁺ efflux, creating a plateau at around an electrochemical potential of +50 mV. This plateau is a component of the effective refractory period, during which the influx of Ca²⁺ also stimulates muscle contraction. No initiation of new action potentials can occur during this period (Absolute Refractory Period).

Repolarization follows in phase three, involving K⁺ efflux through the opening of rapid delayed rectifier K⁺ channels and closing the voltage-gated Ca²⁺ channels.

1.5 Conduction system of the heart

An action potential starts in the SA node. From the SA node, impulses travel to the AV node into a system of conduction fibres that pass through the walls of the atria. At the same time, the electrical signal spreads through the bulk of the atrial muscle (Figure 4).

The impulse reaches cells of the AV node, which transmit action potentials less rapidly than other cells of the conduction system. As a result, the impulse is momentarily delayed by about 0.1 s (called the AV nodal delay) before moving on.

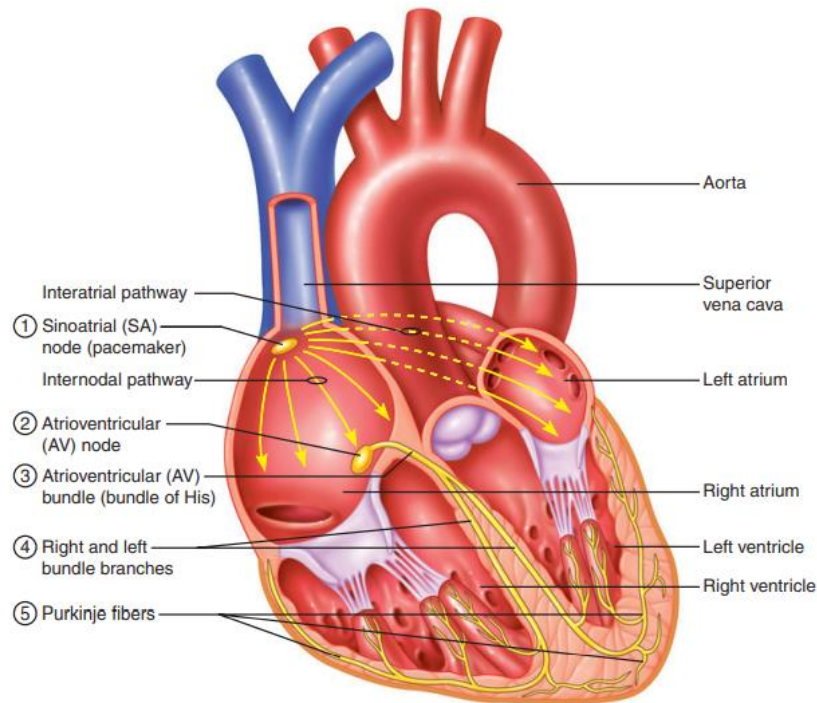


Figure 4: The conduction system of the heart [1]

Then, the impulse travels into the bundle of His, a compact bundle of muscle fibres located in the interventricular septum. The signal advances through the atrioventricular bundle before it splits into left and right bundle branches, which conduct impulses to the left and right ventricles, respectively.

From the bundle branches, impulses travel through an extensive network of branches referred to as Purkinje fibres, which spread through the ventricular myocardium from the apex upward toward the valves. From these fibres, impulses travel through the rest of the myocardial cells.

In a specific situation, the AV node can initiate a heartbeat. As a matter of fact, if the SA node fails to fire an action potential or if it slows down dramatically, the AV node will trigger a new input, which travels through the conducting system and trigger ventricular contraction in the normal manner. The AV node can also control

the heartbeat if conduction between the nodes becomes blocked or slower than it is expected.

1.6 Cardiac Cycle

The cardiac cycle is divided into two distinct periods: diastole (ventricular relaxation), during which ventricular filling occurs, and systole (ventricular contraction), during which the ejection of blood from the ventricles occurs.

This entire phase of blood entering the ventricle is called ventricular filling. First, blood returns to the heart via the systemic and pulmonary veins. Then, it moves into the relaxed atria and passes through the AV valves and into the ventricles under its pressure. The return of blood from the veins to the heart, which is called venous return, occurs because the pressure in the veins is greater than that in the atria. During this time, the pulmonary and aortic valves are closed. Late in diastole, the atria contract, driving more blood into the ventricles. Shortly after that, the atria relaxes and systole begins.

The second phase is an Isovolumetric contraction. At the beginning of systole, the ventricles contract, which raises the pressure within them. When ventricular pressure exceeds atrial pressure, the AV valves close; the semilunar valves remain closed. At this point, blood doesn't flow into or out of the ventricles because all the valves are closed. Phase 2 ends when the ventricular pressure is great enough to force open the semilunar valves so that blood can leave the ventricles.

From this moment, blood is ejected into the aorta and pulmonary arteries through the open semilunar valves, and ventricular volume rapidly decreases. During this phase, referred to as ventricular ejection, ventricular pressure rises to a peak and then begins to decline. When it becomes smaller than aortic pressure,

the semilunar valves close, ending ejection (and systole) and marking the beginning of diastole.

At the onset of early diastole, the ventricular myocardium is relaxing. This phase is an isovolumetric relaxation phase, because all valves are closed, and the blood volume remains constant within the relaxing ventricles. Ventricular pressure is simultaneously too low to keep the semilunar valves open and too high to allow the AV valves to open. Once ventricular pressure decreases to less than atrial pressure blood enters the ventricles from the atria. This event marks the beginning of phase 1, and the pump cycle begins once again.

1.7 Blood pressure

Blood pressure is the measurement of the force due to the pumping action of the heart applied on the walls of the blood vessel. In ideal conditions, the flow law, expressed in equation (1), describes the relationship between blood flow and blood pressure. The flow is directly proportional to the variation of pressure (ΔP) and inversely proportional to resistance at the passage of blood inside blood vessels.

$$Flow = \frac{\Delta P}{R} \quad (1)$$

Blood pressure depends on the volumes of blood that moves to ventricles (Cardiac Output), the compliance, the length and the diameter of blood vessels, the volume of blood and its viscosity.

Blood pressure assumes different names following the site of measurement:

- The Mean Aortic Pressure (MAP) is the average pressure in the aorta throughout the cardiac cycle.

- The Central Venous Pressure (CVP) is the value of pressure in the thoracic veins that lead to the right atrium.
- The difference between the MAP and the CVP is the pressure gradient that drives blood flow through the systemic circuit (ΔP).
- The systolic pressure (SP) and diastolic pressure (DP) are respectively the value of pressure inside the arteria during systole and diastole. SP and DP are the values counted as blood pressure. Average normal values for a healthy individual are 110/70 mmHg.
- Pulse pressure is the difference between systolic and diastolic pressure.

Moreover, the MAP is also expressed by the equation (2).

$$MAP = \frac{SP + (2DP)}{3} \quad (2)$$

The Figure 5 shows the trend of aortic pressure, ventricular pressure and atrial pressure during a cardiac cycle.

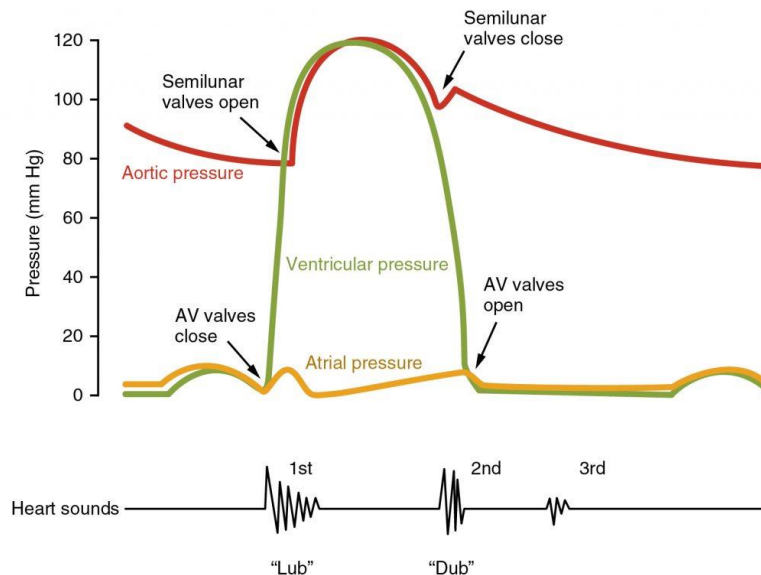


Figure 5: On the top, pressure trend of aortic, ventricular and atrial pressure. On the bottom, the heart sounds.

As the ventricle ejects blood in the aorta, aortic pressure increases to almost that of the ventricle. During diastole, pressure in the aorta goes down because blood continues to flow out. This event causes a slow decline in arterial blood pressure to a minimum just before the next systole.

When the Atrial Ventricular valve is closed, the ventricular pressure rises rapidly, reaches its maximum (120mmHg) and returns to its minimum value when the Atrial Ventricular Valve is open. The pressure inside the atria is almost around lower values (0-15mmHg). Figure 6 summarizes the events of the cardiac cycle and shows its relationship with ventricular volume variations and electrocardiogram.

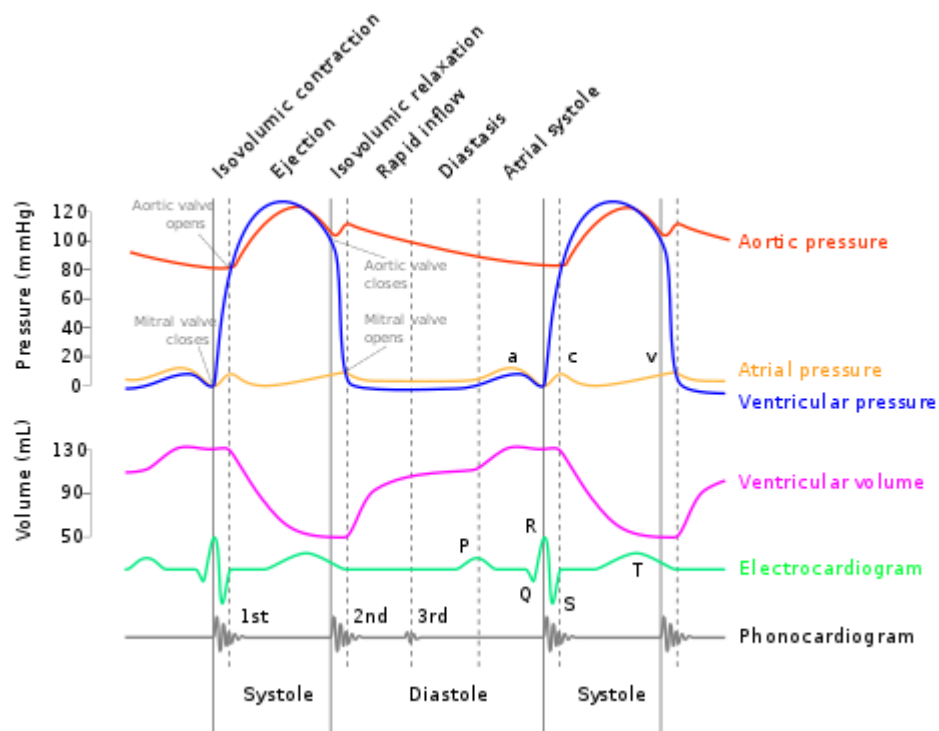


Figure 6: Events of the cardiac cycle: on the top, the waveform of aortic pressure, atrial pressure and ventricular pressure; in the middle, the volume of the ventricle; on the bottom, the electrographic trace and phonocardiogram.

1.8 Arterial blood oxygen saturation

The concept of blood saturation is connected to the capacity of the haemoglobin to bind to oxygen and to realise in the capillaries.

The Hb that let go to bind reversibly to O₂ assumes the name of functional Hb. Most of the Hb in a healthy individual is functional Hb. The functional oxygen saturation (functional SO₂) is the amount of HbO₂ as compared to the sum of oxygenated and reduced haemoglobin.

Another way to define this ratio is to use the concentrations of oxygenated haemoglobin (C_{HbO₂}) and reduced haemoglobin (C_{Hb}). In both cases, the measurement is expressed as a percentage (3).

$$\text{Functional } SO_2 = \frac{\text{HbO}_2}{\text{HbO}_2 + \text{Hb}} \times 100\% = \frac{C_{\text{HbO}_2}}{C_{\text{HbO}_2} + C_{\text{Hb}}} \times 100\% \quad (3)$$

In contrast, dysfunctional Hb does not support the transport of oxygen because it is unable to bind reversibly to oxygen or interfere with the ability of oxyhaemoglobin to release its oxygen to the tissue.

The functional oxygen saturation of explicitly arterial blood is called functional arterial oxygen saturation (SaO₂) and is referred to as functional Hb saturation as well.

2 Physiology of Respiratory System

The respiratory system is responsible for respiration, the process of gas exchange, that occurs at two levels, internal respiration and external respiration. Whereas internal respiration refers to the use of oxygen within mitochondria to generate ATP and the production of carbon dioxide as a waste product, external respiration, or ventilation, refers to the exchange of oxygen and carbon dioxide between the atmosphere and body tissues, which involves both the respiratory and circulatory systems.

2.1 Organs and Structures of the Respiratory System

Functionally, the respiratory system can be divided into a conducting zone, which includes the organs and structures not directly involved in gas exchange and a respiratory zone, which in the gas exchange occurs (Figure 7).

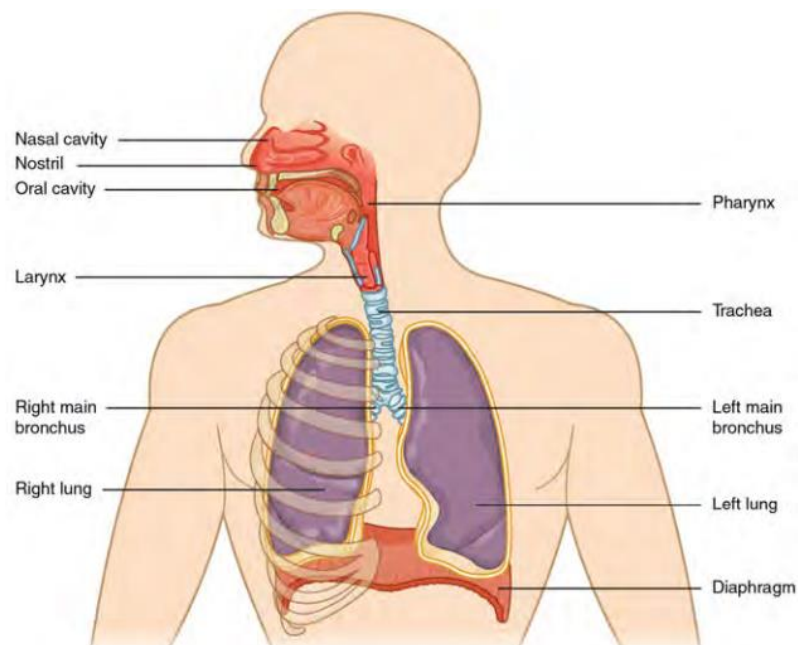


Figure 7: The main structures and organs of the respiratory system

The main functions of the conducting zone are to provide a route for incoming and outgoing air, remove debris and pathogens from the incoming air, and warm and humidify the incoming air. Instead, the respiratory zone includes structures that are directly involved in gas exchange.

In summary, the airways are divided into three zones: the nose, external organ of the respiratory system. Its cavities can filtrate and humidify the airflow and transport it inside the respiratory apparatus; the second part is composed of pharynx, larynx and trachea and the bronchial tree, which is the collective term used for these multiple-branched bronchi. Firstly, it is generated from the division into right and left bronchia, then they branch out into smaller branches, such as alveolar duct, bronchiole and at least alveoli.

The major organs of the respiratory system are the lungs, which are in the thoracic cavity. Each lung is divided into lobes. Air gets into and out of the lungs through the upper airways and a network of tubes forming a system of passageways called the respiratory tract.

2.2 Mechanism of respiration: Ventilation

Pulmonary ventilation consists of the process of inspiration, where air enters the lungs, and expiration, where air leaves the lungs (Figure 8).

Air moves follow a pressure gradient, from an area of high pressure to one of low pressure. Inspiration occurs when the pressure in the alveoli is less than the pressure in the atmosphere, creating a pressure gradient for air to move into the alveoli; expiration occurs when the pressure in the alveoli exceeds the pressure in the atmosphere, creating a pressure gradient that allows air to leave the alveoli.

Four parameters are responsible for ventilation: atmospheric pressure; intra-alveolar pressure, that is the pressure of air within the alveoli; intrapleural

pressure, that is the pressure inside the pleural space; transpulmonary pressure, which is the difference between the intrapleural pressure and the intra-alveolar pressure. The intrapleural pressure is negative (-4 mmHg).

During inspiration, the diaphragm and external intercostal muscles contract, causing expansion of the thoracic cavity and the increase of lung volume. This rise creates a lower pressure within the lung than atmospheric pressure, causing air passages into the lungs.

During exhalation, the diaphragm and intercostals relax, causing the thorax and lungs to recoil. As soon as the pulmonary air pressure is above the atmospheric pressure, the air is forced out of the lungs. However, during forced exhalation, the internal intercostals and abdominal muscles may play in forcing air out of the lungs.

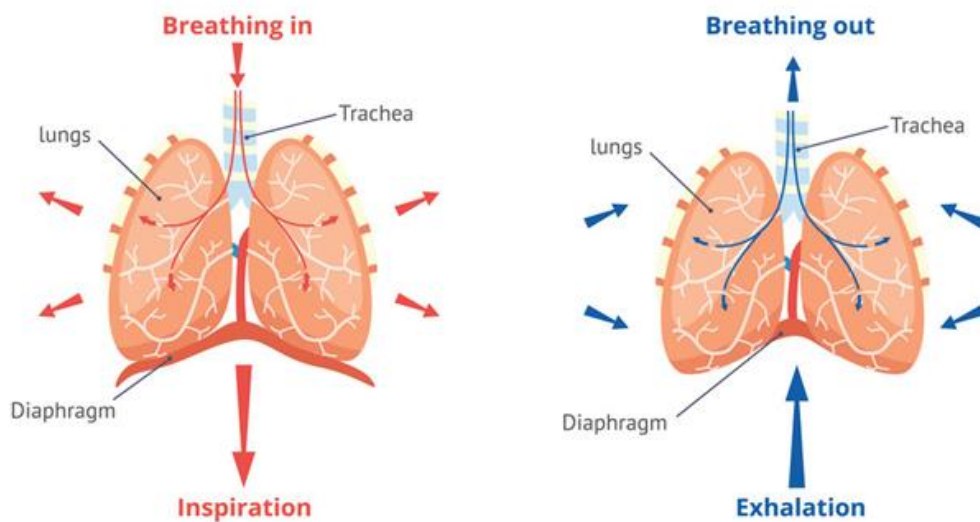


Figure 8: Movements of lungs and diaphragm during Inspiration (on the left) and Exhalation (on the right). The red arrows indicate the movement of air out of lungs, the blue arrows indicate the flow of air outside the lungs.

2.3 Mechanism of respiration: Gas Exchange

Gas exchange occurs at two sites in the body: in the lungs, where oxygen is picked up and carbon dioxide is released at the respiratory membrane, and at the level of tissues, where oxygen is released, and carbon dioxide is picked up. External respiration refers to gas exchange across the respiratory membrane in the lungs. Internal respiration refers to gas exchange across the respiratory membrane in the metabolizing tissues. Gas exchange occurs by diffusion, which is the movement of a substance from a high to low concentration zone. Therefore, energy is not required to move oxygen or carbon dioxide across membranes. Moreover, the anatomy of the lung maximizes the diffusion of gases: the respiratory membrane is highly permeable to gases; the respiratory and blood capillary membranes are thin and the exchange surface area throughout the lungs is large.

2.3.1 Gas Exchange: External Respiration

External respiration occurs due to partial pressure differences in oxygen and carbon dioxide between the alveoli and the blood in the pulmonary capillaries.

Although the solubility of O₂ in blood is not high, there is a drastic difference in the partial pressure of O₂ in the alveoli versus in the blood of the pulmonary capillaries. This difference is about 64 mmHg: the partial pressure of O₂ in the alveoli is about 104 mmHg, whereas its partial pressure in the blood of the capillary is about 40 mmHg. This consistent difference in partial pressure creates a strong pressure gradient that causes oxygen to rapidly cross the respiratory membrane from the alveoli into the blood.

The partial pressure of CO₂ is also different between the alveolar air and the capillary blood (45 mmHg in blood capillaries and 40 mmHg in the alveoli). The partial pressure difference is less than that of oxygen, about 5mmHg. However,

the solubility of CO_2 is much greater than that of O_2 (by a factor of about 20) in both blood and alveolar fluids. As a result, the relative concentrations of oxygen and carbon dioxide across the respiratory membrane are similar.

2.3.2 Gas Exchange: Internal Respiration

Internal respiration is the gas exchange that occurs at the level of body tissues. Similar to external respiration, internal respiration also occurs as simple diffusion due to a partial pressure gradient. However, the partial pressure gradients are the opposite of those present at the respiratory membrane. The partial pressure of O_2 in tissues is low, about 40 mmHg, because oxygen is continuously used for cellular respiration. In contrast, the partial pressure of O_2 in the blood is about 100 mmHg. This creates a pressure gradient that causes oxygen to dissociate from haemoglobin, diffuse out of the blood, cross the interstitial space, and enter the tissue.

Considering that cellular respiration continuously produces CO_2 , the partial pressure of CO_2 is lower in the blood than it is in the tissue, causing carbon dioxide to diffuse out of the tissue, cross the interstitial fluid, and enter the blood. Then it is carried back to the lungs bound to haemoglobin, dissolved in plasma. By the time blood returns to the heart, the partial pressure of O_2 has returned to about 40 mmHg, and the partial pressure of CO_2 has returned to about 45 mmHg. The blood is then pumped back to the lungs to be oxygenated once again during external respiration.

B. Physiological Signal analysis: origin and waveform description

3 Electrocardiographic signal description and acquisition

Electrocardiogram is the recording of electrical force due to contractile activity of the heart. It is a graphical demonstration of the variation of biopotential versus time, recorded on the skin surface.

3.1 Origin of the signal

The depolarization and repolarization of heart cells and their physiological consequences generate the ECG waveform (Figure 9).

During a cardiac cycle, some cardiac cells are negatively charged; other ones are positively charged. This event results in a separation of electrical charges, that generates an electric dipole. This latter one is known as the cardiac dipole, characterized by three different parameters: a moment, an orientation and a direction, that can change in time following the variation of intracellular potential.

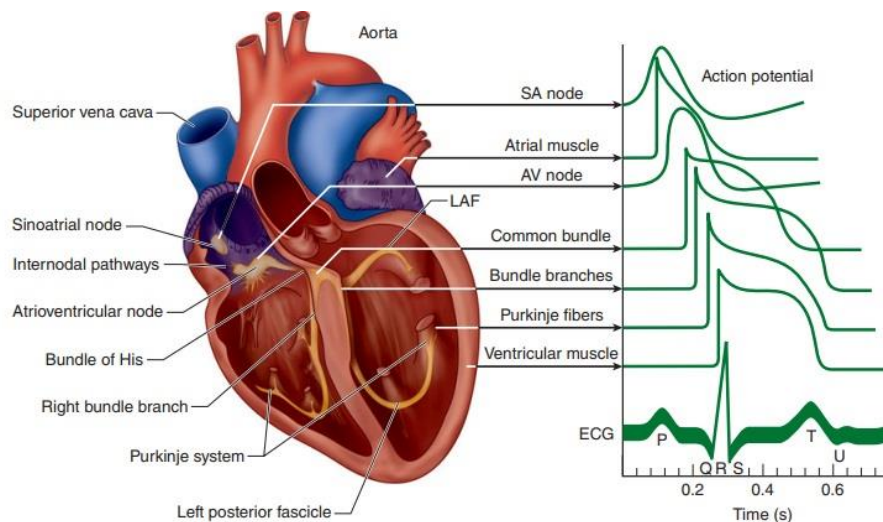


Figure 9: the right panel shows an ECG signal and its formation over time due to the subsequentially spread of action potential in the different regions of the heart.

The cardiac dipole generates a current flux in the surrounding fluid, provoking an electric field that could be detected by electrodes placed in the solution.

This relationship among the direction, the orientation of the current dipole, and the polarity of potentials is critical in electrocardiography. When an electrical wave is moving toward an electrode, it records a positive potential. If an electrical wave is moving away from an electrode, it records a negative potential.

3.2 Signal acquisition

The electrical activity of the heart is the summation of the electrical activity of all heart cells. It can be recorded as changes in the voltage signal appearing on the surface of the body, due to the spread of action potential in myocardial tissue.

The acquisition system includes some electrode, that are applied on the skin and can convert a biological signal into an electrical signal, that is an electrocardiographic potential.

Electrodes are connected to form leads and each lead record the potential difference between two electrodes. The actual potential at either electrode is not known, and only the difference between two electrodes is recorded.

The standard clinical ECG includes recordings from 12 leads, that include three standard limb leads (leads I, II, and III), six precordial leads (leads V1 through V6) and three augmented limb leads (leads aVR, aVL, and aVF).

The position of each lead and electrode are also defined. For standard leads:

- Lead I represents the potential difference between the left arm (positive electrode) and right arm (negative electrode).
- Lead II displays the potential difference between the left leg (positive electrode) and right arm (negative electrode).

- Lead III represents the potential difference between the left leg (positive electrode) and left arm (negative electrode).

The electrode on the right leg serves as an electronic reference that reduces noise and is not included in these lead configurations.

These leads form a triangle, known as the Einthoven triangle (Figure 10). Inside the triangle, the potential in lead II is equal to the sum of potentials that flow to leads I and III.

Precordial leads are also known as unipolar leads because they register the potential at one site respect to an absolute zero potential. The absolute zero potential correspond to Wilson central node or a combination of two limb electrodes. The position of six precordial leads is shown in Figure 11.

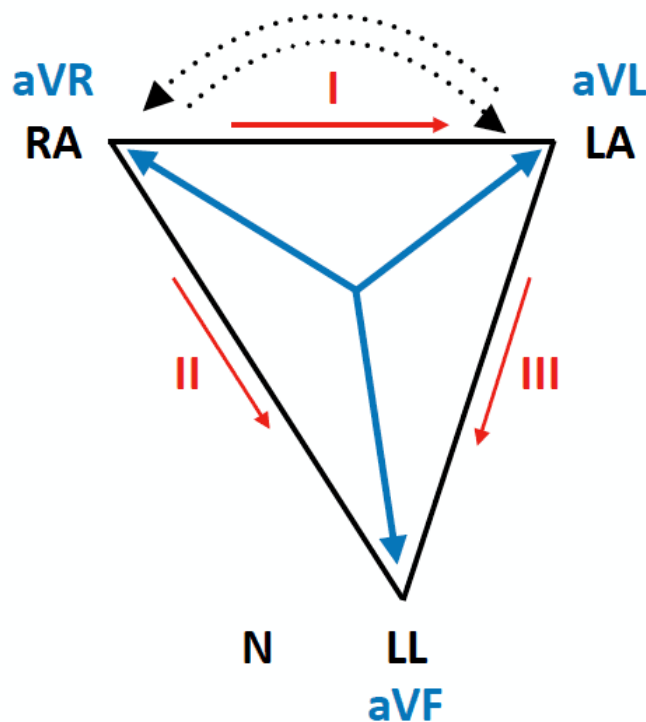


Figure 10: Schematic representation of Einthoven triangle.

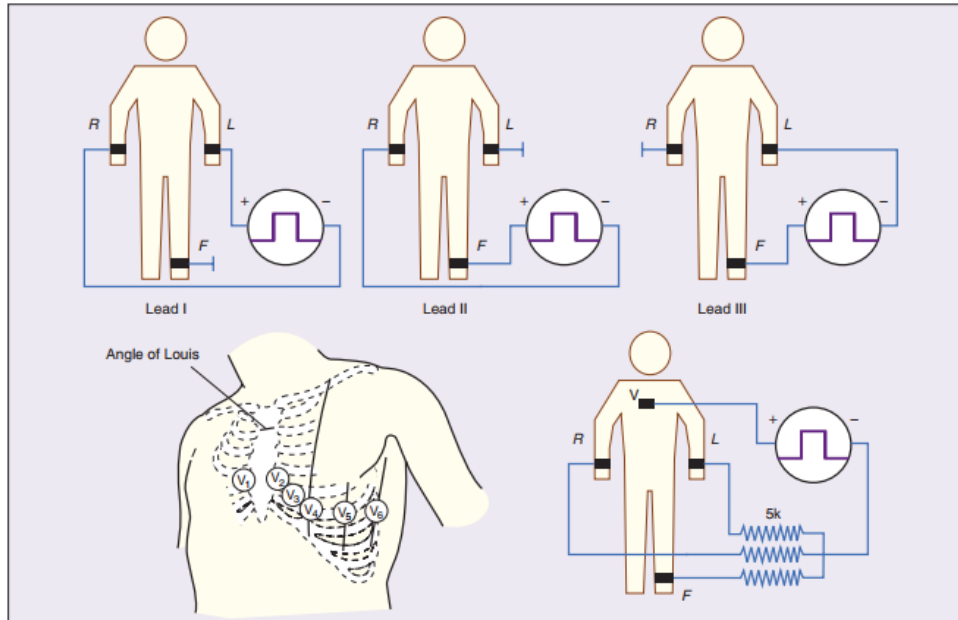


Figure 11: Top panel: Electrode connections for recording the standard limb leads I, II, and III. R, L, and F indicate locations of electrodes on the right arm, left arm, and left foot, respectively. Bottom panel: Electrode locations for recording a precordial lead. On the left, the positions of the exploring electrode for the six precordial leads. On the right, the connections to form the Wilson central terminal for recording a precordial lead [1].

The Wilson central terminal is formed by combining the output of the left arm (LA), right arm (RA), and left leg (LL). The potential in each V lead can be expressed as (equation (4)):

$$V_i = E_i - WCT \quad (4)$$

Where V_i is the potential at the exploring electrode, E_i is the voltage sensed at and WCT is the potential at Wilson central node, expressed as (equation (5)):

$$V_i = E_i - WCT \quad (5)$$

The amplified leads system was designed to produce a larger amplitude signal than if the full Wilson central terminal were used as the reference electrode. The lead aVR refers to right arm electrodes, the left arm electrode is lead aVL, and aVF refers to the left leg electrode. The amplified leads are connected to precordial leads as it is in equations (6), (7) and (8).

$$aVR = RA - (LA + LL)/2 \quad (6)$$

$$aVL = LA - (RA + LL)/2 \quad (7)$$

$$aVF = LL - (RA + LA)/2 \quad (8)$$

Once the ECG signal is collected by electrodes, it is digitalized, amplified and filtered.

3.3 Signal description

The typical ECG signal is showed in detail in Figure 12. Each heartbeat displayed is a sequence of electrical waves characterized by peaks and valleys. ECG mainly provides information in duration and amplitude, which mirror the physiological state of the heart.

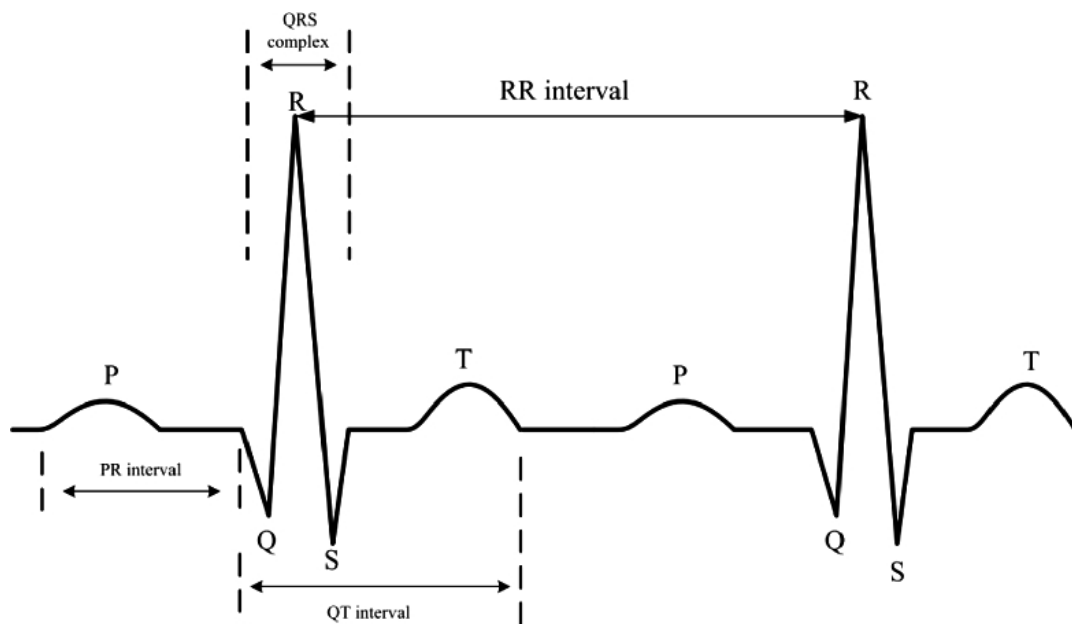


Figure 12: Schematic representation of ECG signal that shows its characteristic picks and segments.

The frequency range of the ECG signal is 0.05–100 Hz and its dynamic range is 1–10 mV.

ECG signal consists of P wave, QRS complex, T wave. P-wave occurs due to the depolarization of the atria. The PQ segment identifies the time of spreading excitement from the atria to the ventricles. The depolarization of ventricles generates the QRS complex. The repolarization of atria is overlapped by the QRS complex. T-wave occurs during the repolarization of ventricles.

The following list sums up the main characteristics of waves in the ECG signal.

- P wave: It is a slow, low amplitude wave, with an amplitude of about 0.1-0.2mV
- PR interval: The PR-interval is measured from the beginning of the P wave to the beginning of the QRS complex, with a duration 120-200 ms.
- QRS complex: The QRS complex is the largest voltage deflection of approximately 1mV. The duration of the regular QRS complex lies between 60ms to 100ms. Duration, amplitude and morphology of the QRS complex are usable in diagnosing cardiac alterations.
- ST segment: It connects the QRS complex and the T wave with a duration of 0.08 to 0.12 ms. The ST segment generally ends at the beginning of the T wave.
- T wave: The amplitude of the T wave is 0.1-0.3 mV; the duration is 120-160ms.
- U wave: In some recordings, the U wave can occur. Its physiological meaning is not so clear.

ECG signals is strictly connected to the cardiac cycle. At first, both the atria and ventricles are relaxed (diastole). The P wave represents the depolarization of the atria, that leads to atrial contraction (systole). Atrial systole extends until the QRS complex when the atria relax. The QRS complex represents the depolarization of the ventricles and is followed by ventricular contraction. The T wave represents

the repolarization of the ventricles and marks the beginning of ventricular relaxation (Figure 13).

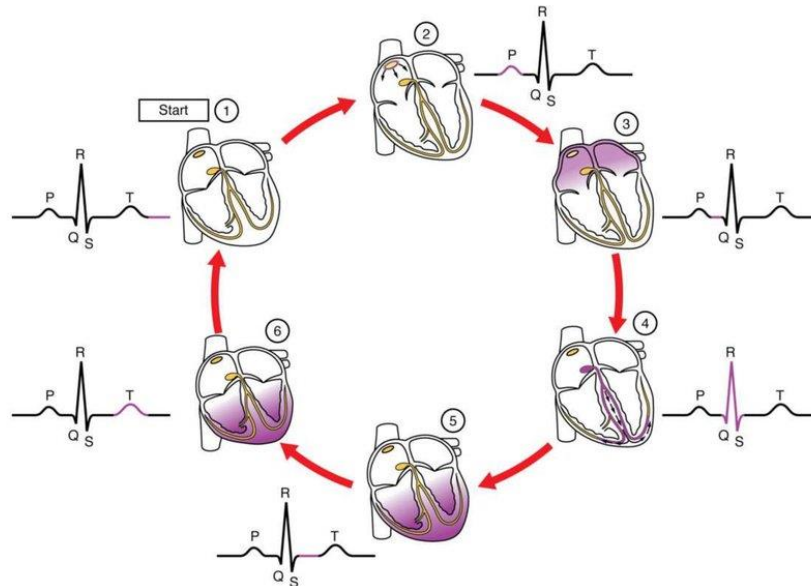


Figure 13: The phases of the cardiac cycle and the genesis of the electrocardiogram. Phase 1: Both atrial and ventricles are relaxed. Phase 2: an electrical impulse travel from the SA node to the atria, causing their contraction. The P wave is generated. Phase 3: The impulse reaches the AV node. Phase 4: the impulse reaches the ventricles, that contract. The QRS complex is generated. Simultaneously, the atria relax. Phase 5: Propagation up the Purkinje fibres. Phase 6: Ventricles repolarize, and a T wave is generated.

4. Photoplethysmography: genesis and description of the signal

Photoplethysmography (PPG) is a non-invasive optical technique used to measure changes in blood volume in microvascular tissue under the skin due to the pulsatile nature of blood.

The word “plethysmography” comes from two Greek words: “plethysmos” means “increase”.

4.1 Origin of the Signal

The waveform of general photoplethysmography is due to absorbance properties of blood, skin and other biological tissue described by Beer-Lambert Law.

Moreover, PPG is based on the properties of light scattering caused by glucose in the blood. The increase in glucose decreases the misalignment of the light beam penetrating the tissue because the refractive index is reduced by its presence. As a result, a smaller amount of light is absorbed, and the light

the intensity which crosses the tissue is greater.

Generally, the Beer-Lambert Law is a relationship between the attenuation of light through a substance and the properties of that substance. This law assumes that the optical attenuation, defined also as Absorbance (A), of a uniform distributed material is proportional to its molar attenuating coefficient (ϵ), its optical path length (l) and to the concentration of attenuating species (c), in accordance to following equation (9).

$$A = \epsilon l c \quad (9)$$

The absorbance is the ratio between the intensity of the incident wave (I_0) and the intensity of transmitted light (I) (equation (10)).

$$A = \log_{10} \frac{I_0}{I} \quad (10)$$

For biological tissue, the modified Beer-Lambert law is used to describe light propagation through human tissue and applied to measure blood volume and oxygenation. The modified law takes into account the contribution of scattering phenomena of biological tissue.

The absorption of light in human blood mainly depends on the concentration of haemoglobin in the blood.

Figure 14 shows the absorption spectra of human blood haemoglobin and oxygenated haemoglobin versus the wavelength of light.

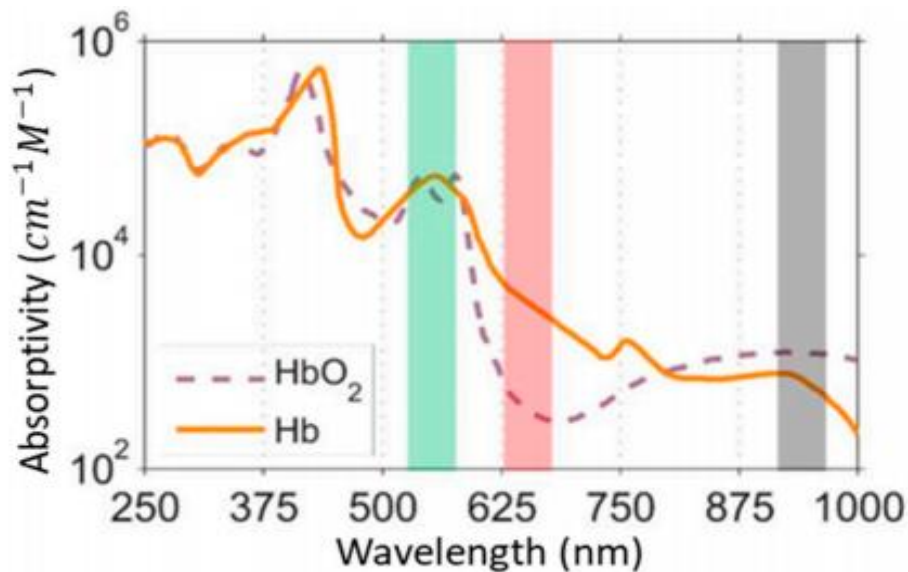


Figure 14: Absorptivity of Hb and HbO₂ respect wavelength. Green region aligns the spectra of green light, red region of red light and grey region of infrared emission.

The penetration depth of the light depends on the wavelength and distance between the light source and photodetector, too.

Green light is usually suitable for the measurement of superficial blood flow in the skin. Light with wavelengths between 500 and 600 nm (the green-yellow

region of the visible spectrum) exhibits the highest modulation depth with pulsatile blood absorption. IR or near-IR wavelengths are better for the measurement of deep-tissue blood flow (Figure 15).

4.2 Signal Acquisition

The fundamental components to form a PPG waveform are a light source, typically a light-emitting diode (LED), which transmits a light signal to the biological tissue and a photodetector (PD) that measures variations in blood volume through a change in light intensity.

The light source emits light to tissues; the photodetector receives the reflected or transmitted light that comes backs from the target tissue. The received light is proportional to blood volume variations and depends on the optical properties of the mediums that the light passes throughout.

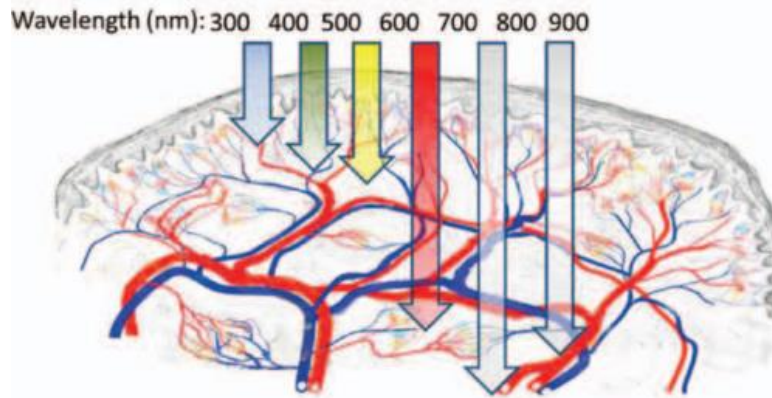


Figure 15: Depth of penetration of different wavelengths.

PPG sensors have two basically configurations: transmission or reflective mode. In transmission modality, a medium, such as a finger, separates the transmitter and the receiver. In the second configuration, the transmitter and the photodetector are located on the same side (Figure 16).

In transmission modality, the LED light passes through skin pigmentation, bone and arterial and venous blood. These biological elements absorb light following their optical properties and transmit an output signal that is received by the detector and quantified by filters and converters. In contrast, a PPG sensor in reflection mode reflects the LED light on the skin, which is received by the detector, and quantified similarly. This configuration is usually applied in the body parts too thick to allow the transmission of light, such as the wrist and forehead.

The outcome of the PPG signal depends mainly on the flow of blood and oxygen to the capillary vessels in each heartbeat. In contrast, bone absorption influences only transmission-type PPG signals. In reflection-type signals, bone absorption is not relevant.

Schematically, the PPG probe consists of the signal coming back to photodetectors, that send a signal to a low pass filter and a high pass filter. Filters are required to remove signal components relative to motion artefacts and the respiration signal. Then the signal is amplified and sent to a microcontroller for consequent manipulation.

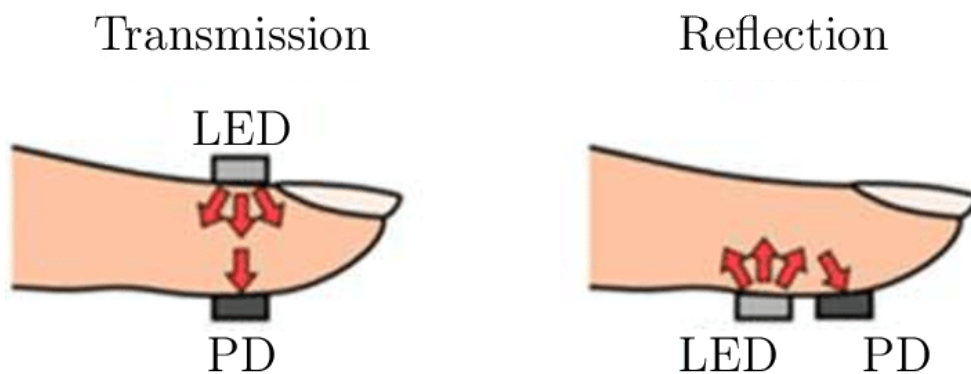


Figure 16: The two possible configurations of a PPG sensor. On the left, the transmission modality, on the right the reflective modality.

4.3 Signal description

The characteristic points of the PPG signal are summarized in Figure 17.

A PPG signal consists of Alternate current (AC) and Direct current (DC) components.

The AC component indicates the change in blood volume, which occurs because of the cardiac function. The DC component indicates light absorption in different layers of the skin.

The AC component is the most relevant to identify interesting parameters about the health state of an individual. The pulsatile component of the PPG signal reflects the cardiac cycle. The AC signal is composed of two phases, the anacrotic phase and the catacrotic phase.

The anacrotic is the rising phase of the pulse during systole; the catacrotic phase is the falling phase of the pulse during diastole. Sometimes, a dicrotic notch can also be found.

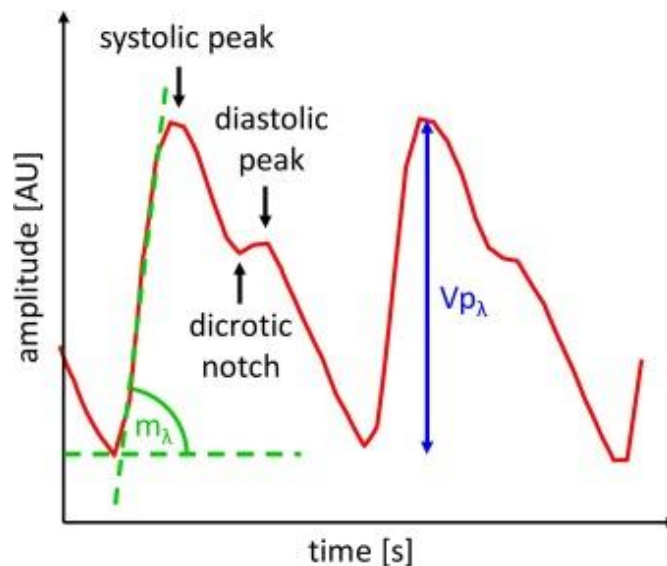


Figure 17: Two cycles of a PPG signal. The highest peak is the systolic peak followed by the dicrotic notch and diastolic peak. For SpO_2 estimation, the slope of the rising edge of the systolic peak m_λ and the height of the peak Vp_λ are needed.

The systolic phase starts with a valley and ends with the pulse wave systolic peak. The pulse wave end shows another valley at the end of the diastolic phase.

Figure 18 displays the AC and DC components of the PPG signal and their physiological meaning.

The frequency range of AC component of signal is about 0.5–4.0 Hz.

4.3.1. Estimation of Arterial Oxygen Saturation

The SpO₂ is an estimation of arterial oxygen saturation. To measure at two wavelengths permits to distinguish the concentrations of only two different absorbers, the oxygenated and reduced haemoglobin.

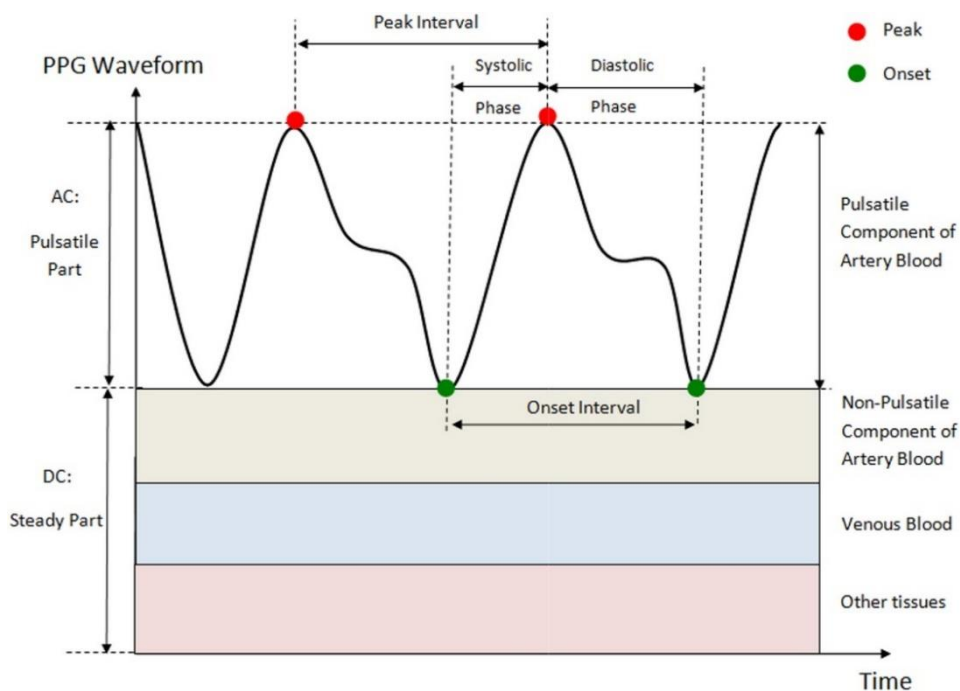


Figure 18: PPG waveform composition: The DC component represents the light absorption of arterial blood (the light-yellow area), venous blood (the sky-blue area), different types of tissues (epidermis, dermis, subcutis, or hypodermis), and the bones (the light-red area). The AC component represents the pulsatile component of Artery Blood. The red point is the systolic peak, the green point is the onset of systolic phase. On the top of figure, there is the division in time of cardiac phases: systolic phase and diastolic phase.

The estimation of SpO₂ is based on the concept that the light absorbance of different species of Hb at different wavelengths is not the same. The associated extinction coefficients¹ for the absorption of light for different wavelengths are

linearly independent with enough variation for adequate sensitivity but not so large that the blood appears opaque to either of the light sources.

For example, the absorbance of light in the red region of the spectrum is much higher for reduced Hb than for HbO₂. The extinction coefficients of both haemoglobin species are equal at the point isosbestic point (805 nm). The reduced haemoglobin is more transparent to light from the infrared region than oxyhaemoglobin.

The algorithm of SpO₂ for a red emitter and infrared emitter includes the following steps:

- The PD collects the transmitted or reflexed signal, due to red and infrared emitters.
- The intensity of the return signals is measured.
- The AC component and the DC component intensities are collected separately through a filtering component.
- The ratio R is calculated as equation (11).

$$R = \frac{AC_{red}/DC_{red}}{AC_{infrared}/DC_{infrared}} \quad (11)$$

- A calibration curve connects the R ratio to SpO₂ estimation. The calibration curve is an experimental curve that can be obtained in different ways.

¹ Extinction coefficient: it is an intrinsic property of chemical species that are dependent upon their chemical composition and structure, and it enhances how strongly a substance absorbs light at a particular wavelength.

5. Heart Rate estimation from photoplethysmography and electrocardiography

Heart rate (HR) is a standard vital sign and has become a routine measurement in healthcare. The monitoring of this signal provides information about the physiologic status by indicating changes in the cardiac cycle.

The HR is a parameter that can be estimated from a PPG and ECG, as both these signals mirror the trend of the cardiac cycle. The HR estimation is based on the identification of the maximum peak of the and on the peak-to-peak interval analysis.

The peak-to-peak measurement is the distance in time between two consecutive systolic peaks for PPG and the distance between two successive R points (RR interval) for ECG. Once the consecutive maximum peaks are identified, different formulas can compute the HR.

The HR is generally expressed in beats per minute (bpm) because it represents the number of beats of the heart in a minute.

Figure 19 shows the waveform of PPG and ECG acquired at the same time.

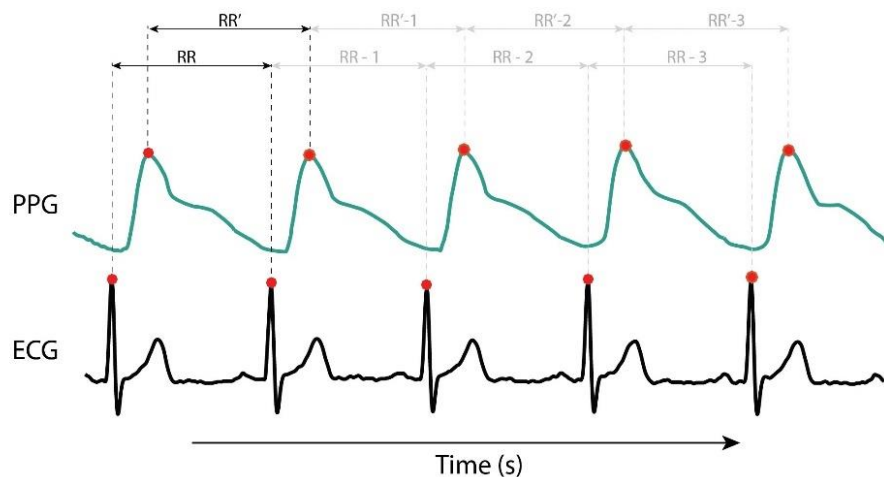


Figure 19: An example of Photoplethysmogram and Electrocardiogram acquired simultaneously. RR' is the distance between two maxima peaks of PPG signal, RR is the distance between two R peaks of ECG signal.

C. State of the art of wearable sensors for daily monitoring

6. Wearable sensors for electrocardiogram

Improvements in sensor knowledge have allowed recording electric impulses from the heart without traditional ECG apparatus. Many of these technologies are wearable and can record cardiac activity for extended periods. This advancement enhances the utility of this technique in the out-of-hospital context. Thank improvement in real-time signal transmission, it is also possible to immediately transmit obtained waveforms for expert interpretation.

Smaller wearable ECG recording devices with differing profiles are now available, including *iRhythm's Ziopatch* and *QardioCore™*, as reported by Pevnick et al. [2] and Sana et al. [3] in their review of 2018 and 2020.

The *Ziopatch* (produced by *iRhythm's*) is an adhesive water-proof patch, applied to the left pectoral region, which provides a single-lead ECG and is used for the continuous monitoring of cardiac rhythms. The patch can be worn at least for 14 days and provides long-term monitoring of cardiac cycles without battery replacement or recharge over this time. Barret et al. [4] assess that over the total wear time of both devices, the adhesive patch monitor detected more events than the Holter monitor. Prolonged duration monitoring for detection of arrhythmia events using single-lead, more comfortable, adhesive-patch monitoring platforms could replace conventional Holter monitoring.

The *QardioCore™* is a wearable device capable of recording up to three ECG channels that pairs with the patient's smartphone or tablet. Data from these devices be sent directly to the physician or uploaded and viewed on a phone app. Several studies report the use of this device during daily activities and its outcomes are compared with a traditional ECG Holter.

7. Wearable sensors for Photoplethysmographic signal

Wearable monitoring devices have attracted considerable consumer interest over the past few years. The rapid demand growth for continuous, portable and chip instrumentation to monitor vital signs encourages the advancement of wearable sensors. The diffusion of them is also supported by technological developments in sensor technology and wireless communications.

The popularity of the PPG technology as an alternative heart rate monitoring technique has recently increased, mainly due to the simplicity of its set-up, the wearing comfortability for its users, its low cost and recently interest in the optical sensor. Nowadays, optical sensors are commonly used to study blood properties, such as viscosity, composition, fluidity. Modern optical scanning technologies take into account the fluid and corpuscular elements of blood, its scattering properties and its chemical composition.

Firstly, PPG sensors were applied in Pulse-oximetry, a typical device used for monitoring arterial oxygen saturation. Pulse-oximetry has revolutionized the monitoring of oxygenation in a continuous, accurate, and non-invasive approach. However, the prototypes of pulse-oximeter are not wearable devices, so people can't use them in daily activities.

Moreover, the first PPG sensors used mainly emitters in the range of infrared or red emission and generally work in transmission modality. The upgrade in optical technologies, in particular the spread of the use of LED components, and the recent improvement in studying optical properties of different species of Hb, allows new solutions in the sensor's design. Nowadays, a green emitter usually substitutes the infrared one.

As a matter of the fact, Castaneda et al. [5] consider green LED the most spread because it penetrates more deeply into tissue and therefore can provide more

accurate measurements. Moreover, in 2020 Banik et al. [6] have developed a wearable reflection-type system to acquire PPG signals and measure pulse rate and SpO₂, achieving accuracy greater than 98%.

The last study refers to research about the comparison of different wavelengths for the PPG sensor design of Hossain et al. [7], which confirms that the green-red couple obtains the greatest accuracy in SpO₂ estimation. IR light has been used in PPG devices for some time because of its penetration power. However, green-wavelength PPG devices are becoming so popular due to the large intensity of variations observed during the cardiac cycle for these wavelengths.

Tamura et al. [8] assume that green is therefore the best choice for heart rate measurement applications, although red and infrared can be successfully used in body locations with a higher concentration of arterial blood (fingertips, ears, and forehead). Light with longer wavelengths (from red to infrared) can be used for pulse oximetry applications. Their considerations are based on interesting paper about optical characteristics and penetration depth of light, written by Anderson and Parrish [9].

7.1 Sources of errors in Photoplethysmography recordings

The main difficulties in using PPG-based monitoring techniques are their inaccuracy in tracking the PPG signals during daily routine activities: PPG signals are very susceptible to Motion Artifacts caused by voluntary and accidental movements and respiratory signals. Moreover, alternative factors such as environmental noise due to light sources may also affect the acquisition, which consequently affects the accuracy of the estimated parameters.

Some recent studies integrate algorithms to eliminate Motion Artefact in PPG design to obtain a satisfying noise to signal ratio [8] [10]. Another possible solution

includes accelerometer or gyroscope to detect the frequencies of motion and to remove them [6].

In case of SpO₂ estimation, the most relevant errors in measurements are due to Hb species that are not involved in O₂ transport but react with transmitted signal at the same wavelength of Hb and HbO₂.

7.2 Body location for Photoplethysmography sensors

PPG outcomes are sensitive to the body location of sensors. In the past decade, PPG devices were located on the earlobe, finger and forehead because of their higher vascularization and the possibility to work in transmission modality.

Tamura [8] reports that PPG sensors are applied on the ring finger and the wrist in recent years.

Nevertheless, the most common commercially available PPG sensor is based on finger measurement sites because finger sites are easily accessible and provide a good signal. Nowadays, wristwatch-type pulse oximetry and blood pressure sensors have been developed and commercialized by several companies. These devices are not usually used in clinical settings, even if they are easier to wear and to use.

Forehead sensors have shown high sensitivity to pulsatile signal variations compared with other peripheral body locations. The thin skin layer of the forehead allows light to come back to the PD rapidly. Moreover, forehead sensors have been shown decreased motion artefacts errors during physical activity.

Forehead and finger type devices result uncomfortable for customers in daily activities. Forehead and finger type device result uncomfortable for customers in daily activities.

D. Device development

8. Consideration behind the development of the device

The fundamental idea is to realize a new device that is wearable, easy to use, wireless and, at the same time, accurate and precise, that can acquire and store a PPG and an ECG at once.

As it has to be used for a long period, the device should be comfortable and quite small. It should have high sensitivity for physiological signals, even if significant noise corrupts the acquisition. Moreover, it might have a battery that has a sufficient duration, doesn't require to be substituted and can be recharged at home.

The features of signals to record were the second fundamental aspect in the process of design. First, an electrocardiogram registers the differential potential between a positive and a negative pole; thus, every exploiting electrode might not be applied to the equal body location. On the other side, PPG sensors require a region of the body with high perfusion and, photodiode and LEDs should be on the same side to make the device less cumbersome.

Considering these conditions, a single-lead ECG (the lead I) and a PPG sensor in reflective modality are the best solutions because these sensors can be embedded into a band or in a patch on the wrist or the torso.

The first idea was to realize an adhesive patch applicable on the torso. Some paper about *ZioPatch* and *QardioCore™* highlights the high precision to detect the heart rate through single-lead ECG on the torso. On the contrary, some considerations, finding in the literature, about the PPG sensor device on the torso suggest that this region produce a low signal to noise ratio. This region presents significant light interference produced by the numerous biological tissues that

light passes through and lower perfusion than peripheral body zones, such as fingers or ear lobes.

For all these regions, a wristband will be the most appropriate case of the device board.

The selected PPG sensor includes one infrared LED, one red LED and two green LEDs. This choice is based on the analysis of literature mentioned in the previous chapter and on the decision to compare the estimation of O₂ saturation through two solutions: red LED /infrared LED vs red LED / green LED.

In the first moment, the PPG and ECG will be acquired not at the same time to test the quality of the signals individually. The sensor of PPG has to be in contact with the skin; one of the electrodes for ECG acquisition will stay on the same side of the optical sensor, the second electrode will be on the opposite side of the case of the device.

Once a person wears the wristband on the left wrist, the acquisition of PPG does not require any action of the subject because the firmware of the device control it. On the contrary, the ECG recordings need that the subject sits quietly for all the pre-determined period, and he has to place a finger of the right hand on the electrode that is not already in contact with the skin.

9. Components of the device

The device prototype includes an optical sensor for PPG, a biopotential sensor for ECG, and a sensor to measure the temperature (Figure 20 and Figure 21). All of them are integrated on the same board. The board also includes a recharged battery (3.7 V), a Micro Control Unit (MCU), Wi-fi card.

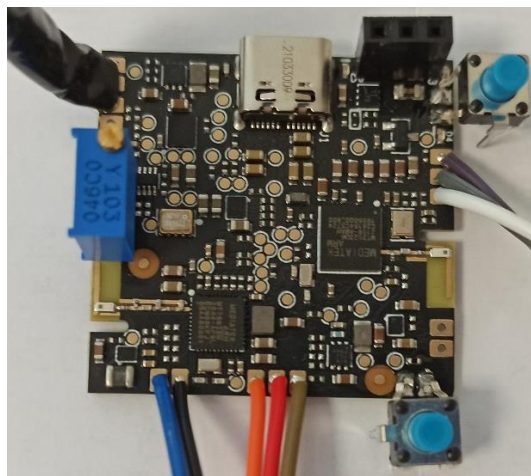


Figure 20: Board of Prototype - Bottom view

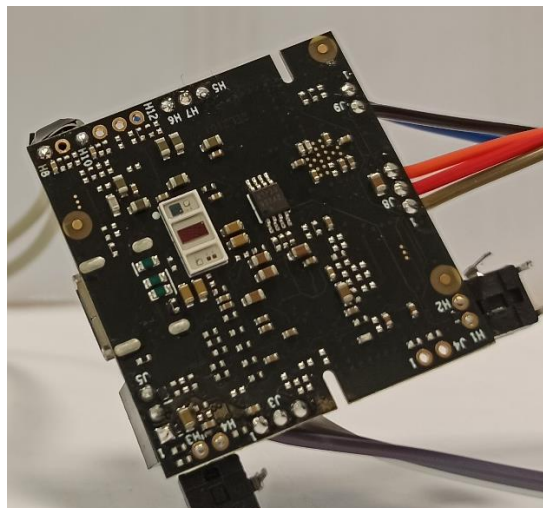


Figure 21: Board of Prototype - top view

The sensor for ECG signal is *Max30001* of *maxim integrated™*. The *Max30001* is a biopotential and bioimpedance, analogue front-end solution for wearable applications. It is a single biopotential channel providing ECG waveforms. The bioimpedance channel includes an integrated programmable current drive, works with common electrodes, and has the flexibility for 2 or 4 exploiting electrodes. The bioimpedance channel also has AC lead-off detection.

The PPG sensors are integrated into *Max86141* of *maxim integrated™*. The *Max86141* is an ultra-low power, completely integrated, optical data acquisition system. On the transmitter side, the *Max86141* have three programmable high-current LED drivers that can be configured to drive up to six LEDs. On the receiver side, the *Max86141* has two optical readout channels that can operate simultaneously. Thus, the device will acquire PPG signal in reflective modality.

The PPG sensors is BIOFY® SFH 7072 of Osram. It integrates two green LEDs (with a peak wavelength of 526 nm), one Red LED (with a peak wavelength of 660 nm) and one Infrared LED (with a peak wavelength of 950 nm). Two photodiodes are also present. A driver controls green and red LEDs, while the second drive controls the infrared one.

The MCU is the MT2523DA of *MediaTek®*, designed for IoT applications and equipped with flexible pin assignments for custom applications.

Max30001 and *Max86141* were tested on two developing boards (Figure 22 and Figure 23) before producing the board prototype to be embedded in the final product.

Three exploiting electrodes are connected on the board; one of them represent the body Bias. Its functionality can be enabled or not from a control action.

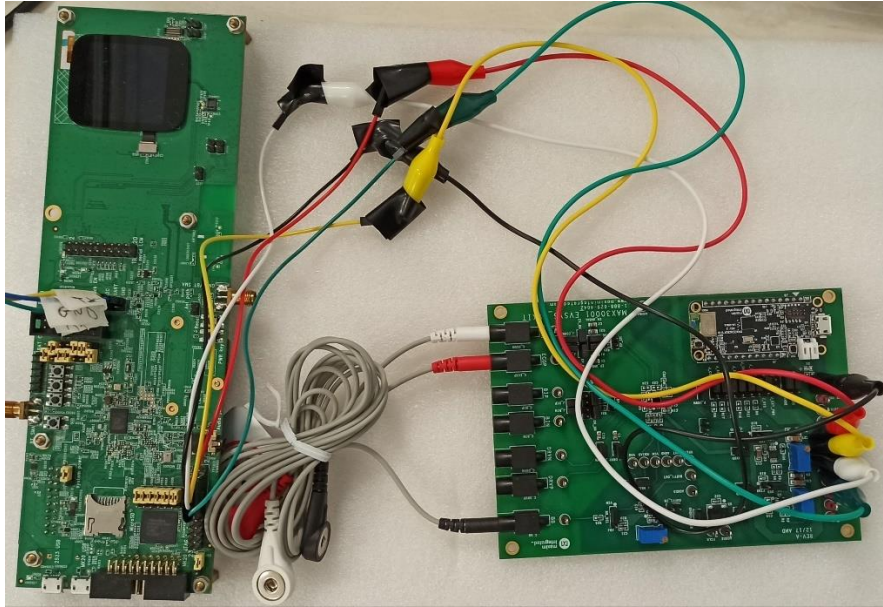


Figure 22: Developing board of ECG sensor



Figure 23: Developing Board of PPG sensor

10. Testing protocol of basic operations of the device

Before applying a rigorous protocol of validation of signals, each sensor was tested autonomously.

The preliminary tests of both sensors include the following steps:

- Control of correct alimentation of the sensor
- Control of correct configuration of the sensors
- Control of Bluetooth transmission modality
- Valuation of the acquired signal.

The first step is necessary to verify if each sensor receives enough alimentation under the technical specification reported on the datasheet of each sensor. Moreover, it's also important to verify if no energy losses occur between the input and the output of the sensors.

The block diagrams in Figure 24 resume the second step for ECG and PPG.

As soon as the ECG acquisition system is switched on, the SPI (Serial Peripheral Interface) initialization occurs. Then control feedback assures that the registers are already configured before that acquisition starts. The *Max30001* collects the biopotential on the skin and produce a signal that travels to the board. Then the signals flow to a client through a Bluetooth connection.

For PPG, the acquisition protocol is almost the same. It's important to note that the *Max86141* is not the actual sensor for this signal. Instead, it is a driver that controls the frequency of the emission, the simultaneously or delayed emission of LEDs of SFH 7472 sensors, the timing of the acquisition.

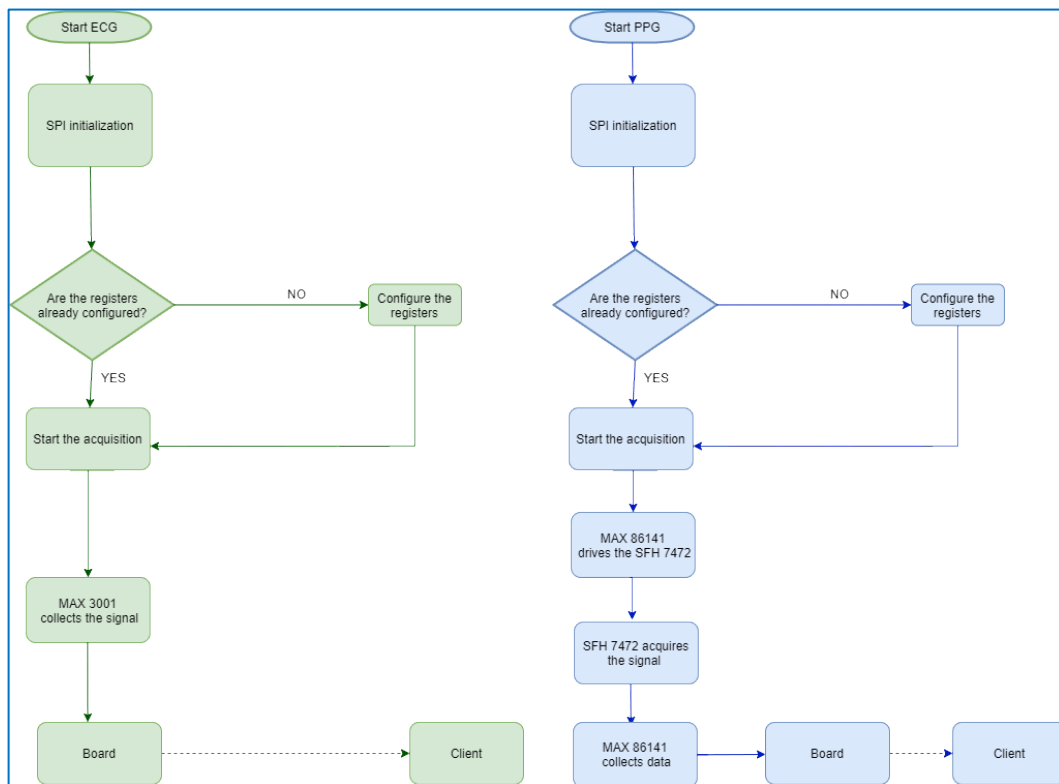


Figure 24: Block Diagram of Electrocardiogram acquisition on the left. Block Diagram of Photoplethysmography acquisition on the right.

The third step is fundamental to be sure that no losses of information occur in the communication of the data. The Bluetooth can transfer tot byte for seconds to the client. The size of transmission influences the choice of the sampling frequency of the two signals. In a realistic situation of usage of the device, the ECG and PPG signal will be acquired and consequently transmitted at the same time.

The fourth step is a primary valuation of the goodness of acquired signals to be sure that these signals have a physiological meaning and a waveform similar to the predicted one.

11. Testing protocol for sensors: background.

As mentioned previously, the two sensors were tested on a developing board before producing the prototype.

This phase is fundamental to establish if the chosen sensors are adequate for the goals of the device, such as the acquisition of a significant signal. Moreover, each sensor should have a high signal to noise ratio, the ability to follow up physiological events of the human body, and adequate characteristics for further manipulation, such as the extraction of some physiological parameters.

In the developing board, the PPG sensor includes one LED that emits a beam only in the region of green light, around 525 nm. During the phase of experimentation, the PPG sensor was substituted with the multiwavelength sensors of Osram.

The acquired signals were transmitted through Bluetooth connection.

11.1 Experimental set-up for Electrocardiography

The prototype board was tested on healthy voluntaries.

The protocol of experimentation consists of a series of acquisitions at different settings. Table I reports a summary of the tests. An alphanumeric code identifies every subject, the letter is M for men, F for woman, the number is unique for a subject. The letter S stay for Simulator, an electrical instrument that simulate the ECG signal.

The raw data are post analysed on MATLAB®. A Fast Fourier Transform (FFT) was applied to the signal to observe and identify the location of noise in the frequency domain.

ID subject	Acquisition System	Position of electrodes	Sampling frequency	Numbers of acquisitions	Body Bias
S1	Developing board		200	2	no
S1	Developing board		500	2	no
M3	Prototype	wrist-wrist	500	6	no
M3	Prototype	wrist-finger	500	4	no
M3	Prototype	wrist-finger	200	3	yes
M1	Prototype	wrist-wrist	200	2	no
M1	Prototype	wrist-finger	500	2	no
M1	Prototype	wrist-finger	200	3	yes
M2	Prototype	wrist-wrist	200	3	yes
M2	Prototype	wrist-finger	200	7	yes
F3	Prototype	wrist-wrist	200	1	no
F3	Prototype	wrist-wrist	500	2	no
F2	Prototype	wrist-wrist	200	5	no
F2	Prototype	wrist-wrist	500	6	no
F1	Prototype	wrist-wrist	200	6	no

Table 1. Settings of hardware and subjects involved for Electrocardiogram acquisitions.

In the first acquisitions, the sampling frequency was 500 Hz or 200 Hz. Then, considering that the signal is transmitted through Bluetooth, the sampling frequency was 200 Hz to reduce the size of sent data.

The testing electrodes are the most diffuse in commerce, without the gel patch. In the case of wrist-wrist and wrist-finger acquisitions, every subject was sitting quietly, with the feet on the floor and the arms were on the chair, parallel to the floor, while the subject lied down for chest acquisitions.

In the last acquisitions, the design also includes the body bias electrode, which reduces the external noise.

On MATLAB®, a Butterworth low pass filter at 40 Hz and a high pass filter at 0.8 Hz are implemented to compare filter and not filter signals.

Moreover, an algorithm identifies R peaks and calculate the Heart Rate.

The acquisition on people were done with the prototype, while the data of simulator are acquired with the developing board.

11.2 Experimental set-up for Photoplethysmography

The first acquisitions of PPG signals were done in reflective modality, with a sensor that includes one green LED. The sensor was applied on a finger and on the wrist. The acquisition time is always 10 seconds on one healthy volunteer.

The sampling frequency was 128 Hz, and no filters are applied on the hardware.

12. Results

12.1 Electrocardiogram

The Table II sums up the value of Signal to Noise Ratio and Heart Rate for every acquisition.

For each subject, the plot of one acquisition is reported in two modalities: raw data and filtered signal.

Subject	Electrodes Position	Acquisition Number	Signal to Noise Ratio (db)	Heart Rate (bpm)	Gain (V/V)	Body Bias
F1	wrist-wrist	1	1	67	1	No
F1	wrist-wrist	2	5	68	1	No
F1	wrist-wrist	3	4	67	2	No
F1	wrist-wrist	4	4	68	2	No
F1	wrist-wrist	5	3	69	2	No
F1	wrist-wrist	6	1	65	2	No
F2	wrist-wrist	7	2	69	2	No
F2	wrist-wrist	8	3	77	2	No
F2	wrist-wrist	9	2	67	2	No
F2	wrist-wrist	10	0	67	2	No
F2	wrist-wrist	11	4	70	2	No
F2	wrist-wrist	12	4	69	2	No
F2	wrist-wrist	13	2	62	2	No
F2	wrist-wrist	14	3	68	2	No
F2	wrist-wrist	15	2	72	2	No
F2	wrist-wrist	16	4	76	2	No
F2	wrist-wrist	17	1	70	2	No
F3	wrist-wrist	18	1	74	2	No
F3	wrist-wrist	19	2	73	2	No
F3	wrist-wrist	20	0	72	2	No
M1	wrist-wrist	21	1	73	1	No
M1	wrist-wrist	22	2	69	1	No
M1	wrist-finger	23	1	70	4	Yes

Subject	Electrodes Position	Acquisition Number	Signal to Noise Ratio (db)	Heart Rate (bpm)	Gain (V/V)	Body Bias
M1	wrist-finger	24	1	80	4	Yes
M1	wrist-finger	25	1	69	4	Yes
M1	wrist-finger	26	1	74	4	Yes
M1	wrist-finger	27	1	67	4	No
M2	wrist-wrist	28	6	82	4	No
M2	wrist-wrist	29	9	81	4	No
M2	wrist-wrist	30	1	83	4	No
M2	wrist-finger	31	16	77	4	Yes
M2	wrist-finger	32	8	74	4	Yes
M2	wrist-finger	33	5	78	4	Yes
M2	wrist-finger	34	2	73	4	Yes
M2	wrist-finger	35	3	69	8	Yes
M2	wrist-finger	36	1	75	4	Yes
M2	wrist-finger	37	9	74	4	Yes
M3	wrist-wrist	38	5	77	2	No
M3	wrist-wrist	39	2	77	2	No
M3	wrist-finger	40	1	83	4	No
M3	wrist-finger	41	1	81	8	No
M3	wrist-finger	42	1	84	16	No
M3	wrist-finger	43	1	83	4	No
M3	wrist-wrist	44	1	82	4	No
M3	wrist-wrist	45	11	82	4	No
M3	wrist-wrist	46	5	77	4	No
M3	wrist-wrist	47	9	81	4	No
M3	wrist-finger	48	8	76	8	Yes
M3	wrist-finger	49	1	75	8	Yes
M3	wrist-finger	50	1	71	8	Yes

Table III. Settings of hardware and subjects involved for Electrocardiogram acquisitions.

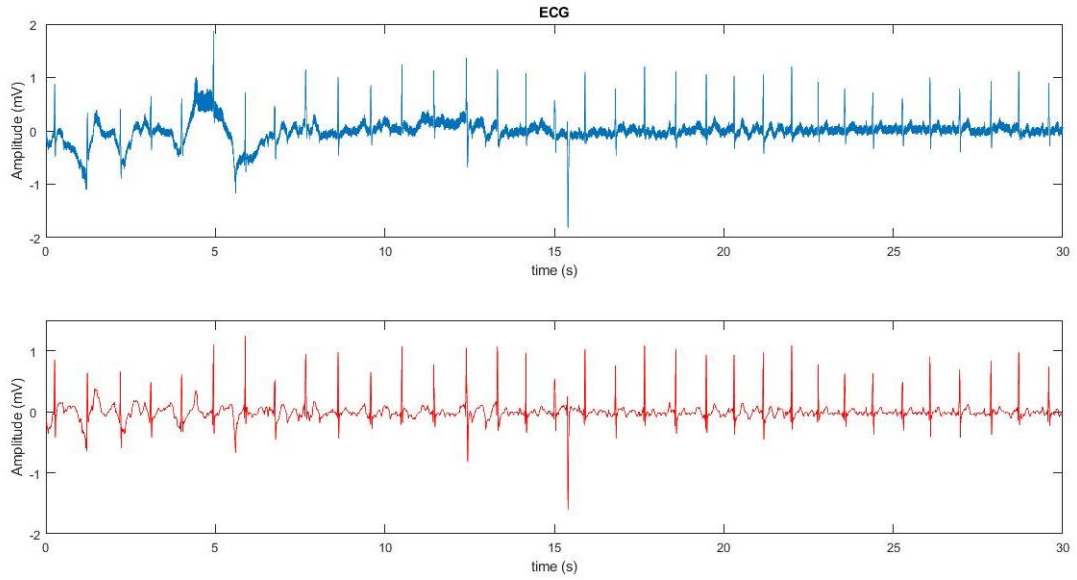


Figure 25: Subject F1, acquisition 3 - On the top, the raw data, on the bottom the filtered signal.

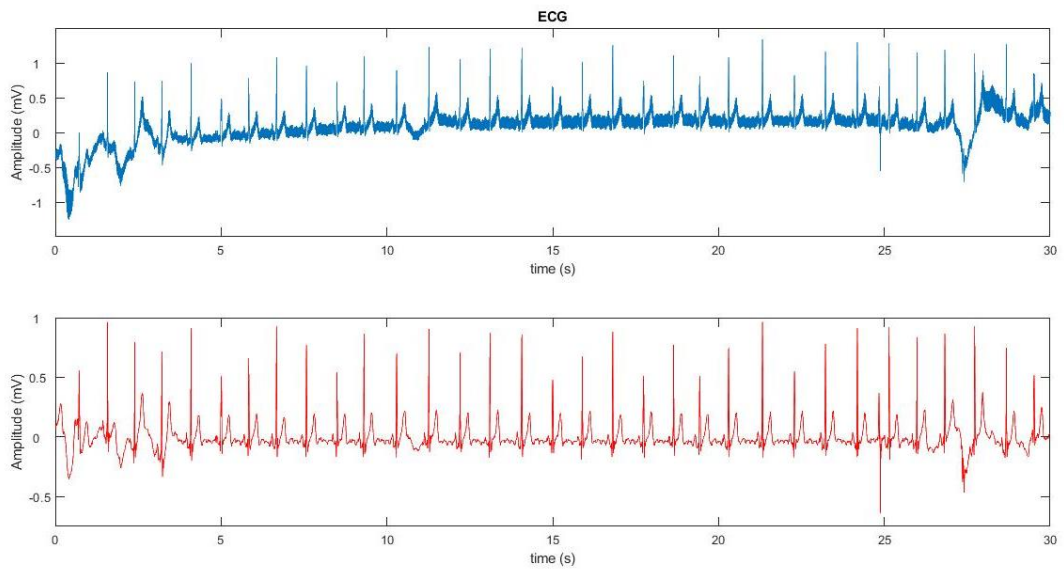


Figure 26: Subject F2, acquisition 9 - On the top, the raw data, on the bottom the filtered signal.

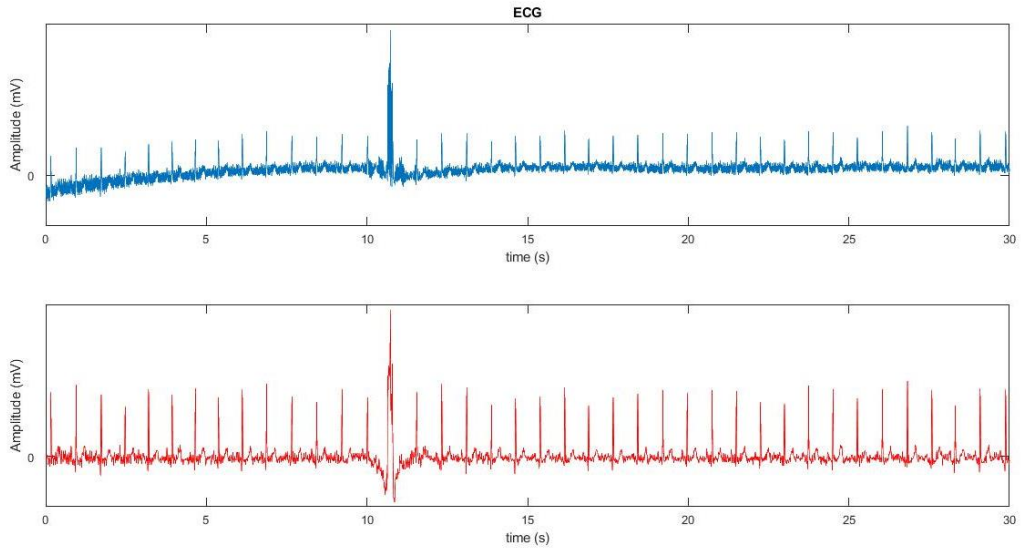


Figure 27: Subject F3, acquisition 20 - On the top, the raw data, on the bottom the filtered signal.

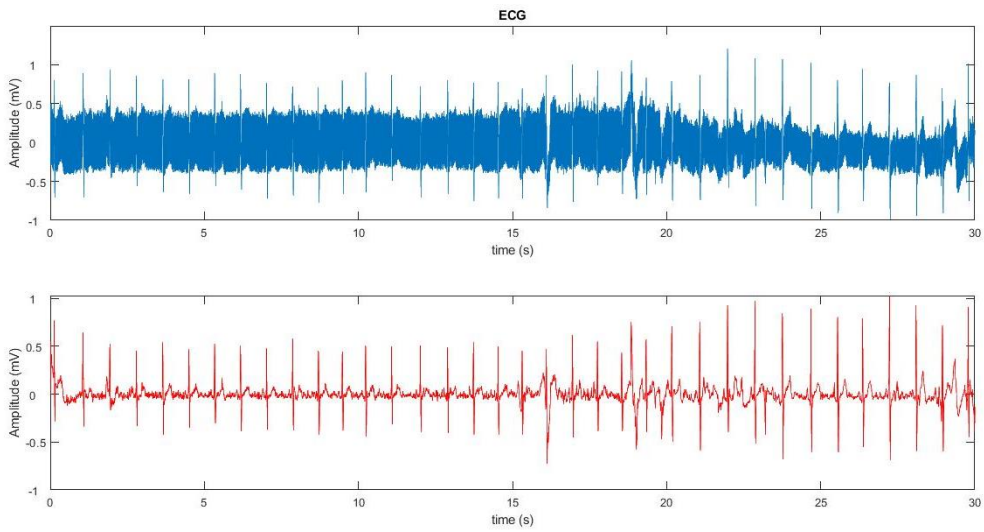


Figure 28: Subject M1, acquisition 22 - On the top, the raw data, on the bottom the filtered signal.

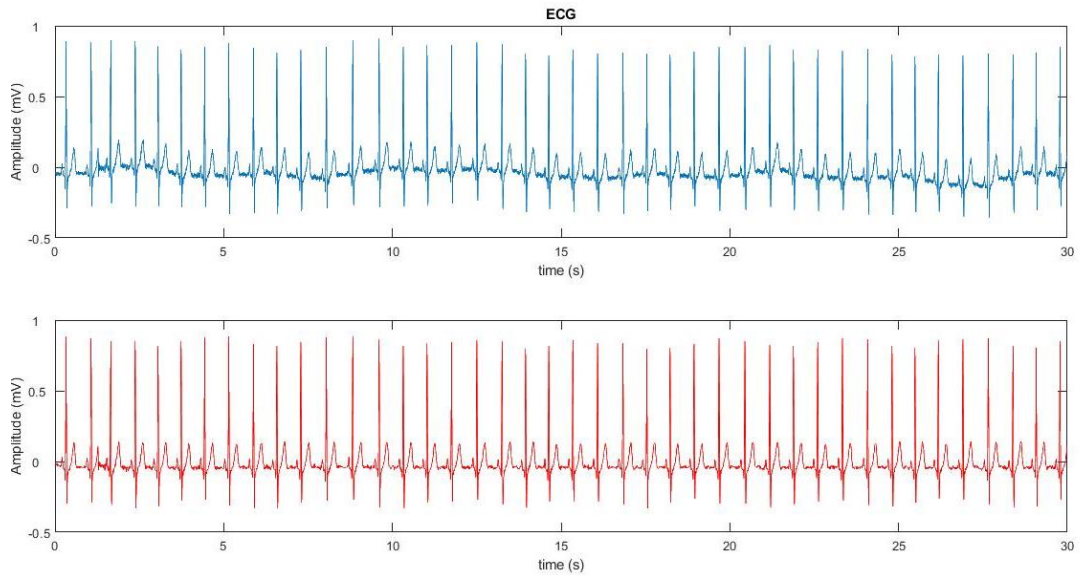


Figure 29: Subject M2, acquisition 29 - On the top, the raw data, on the bottom the filtered signal.

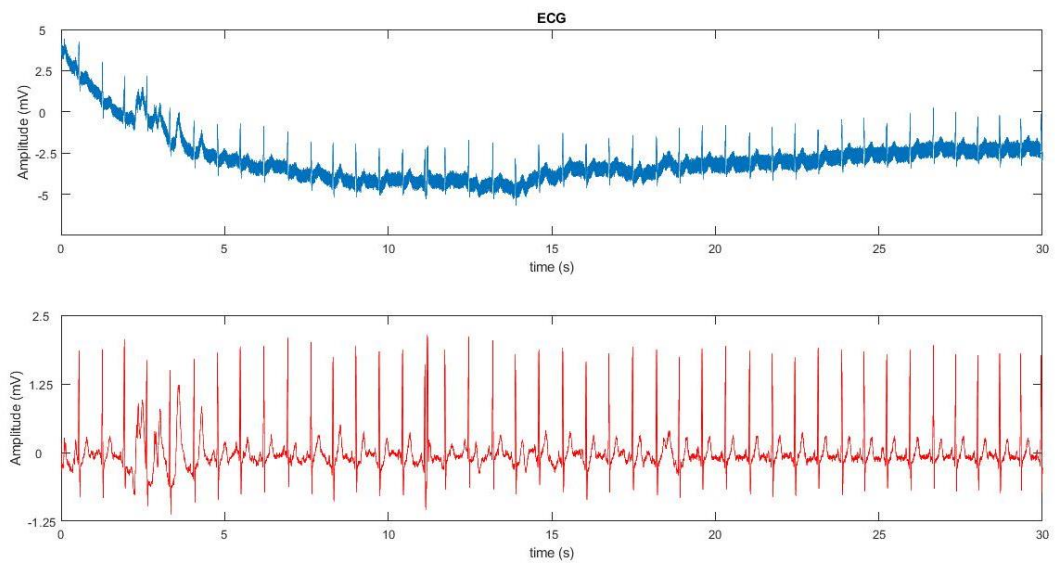


Figure 30: Subject M3, acquisition 40 - On the top, the raw data, on the bottom the filtered signal.

12.2 Photoplethysmography

The following graphs show the PPG waveform, acquired by green LED transmitter and two photodiodes in function sample vector.

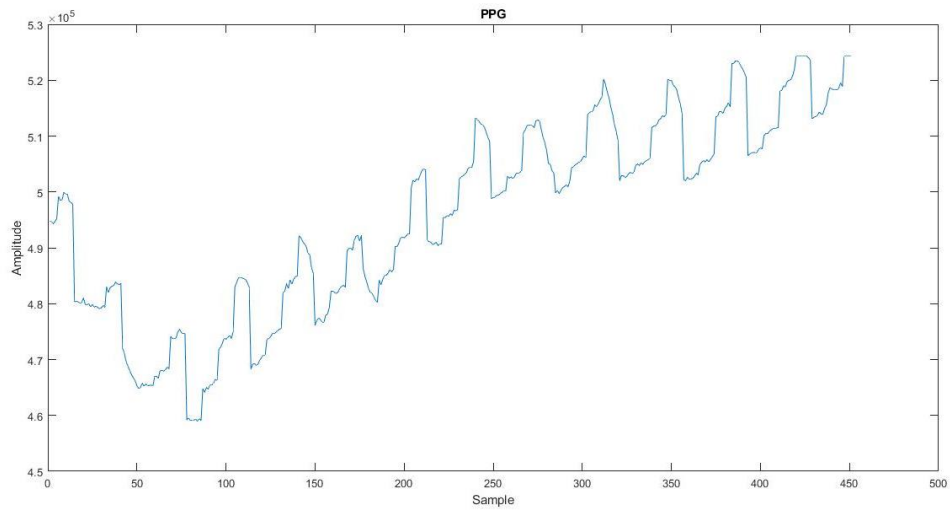


Figure 31: Raw data of PPG signal - acquisition 1

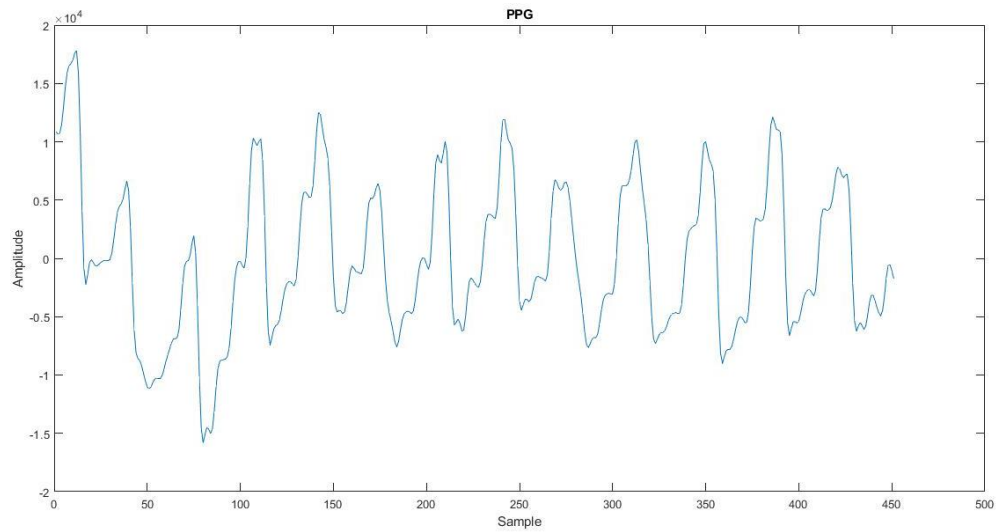


Figure 32: Filter PPG - acquisition 1

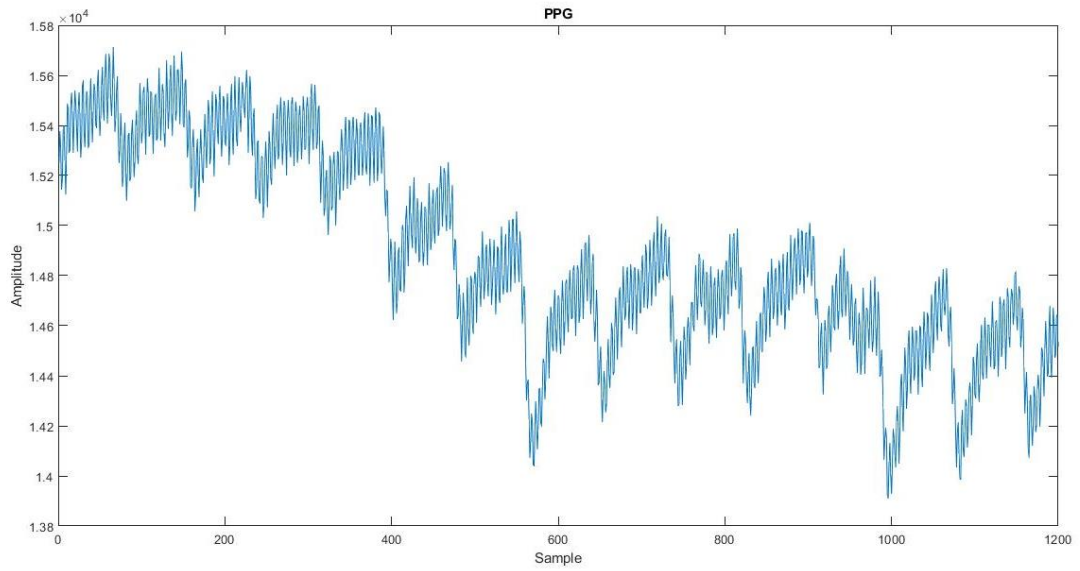


Figure 33: Figure 34: Raw data of PPG signal - acquisition 2

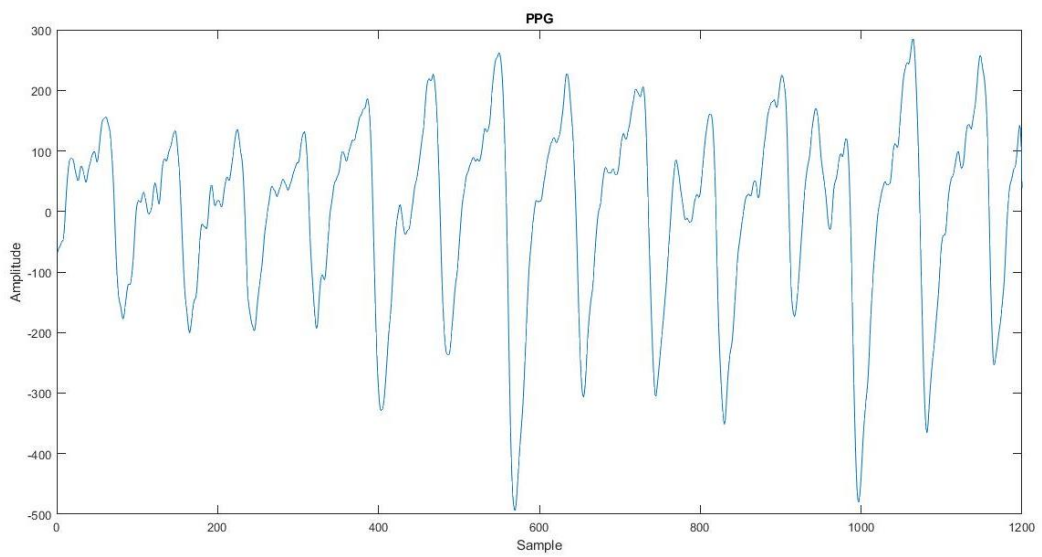


Figure 35: Filter PPG signal - acquisition 2

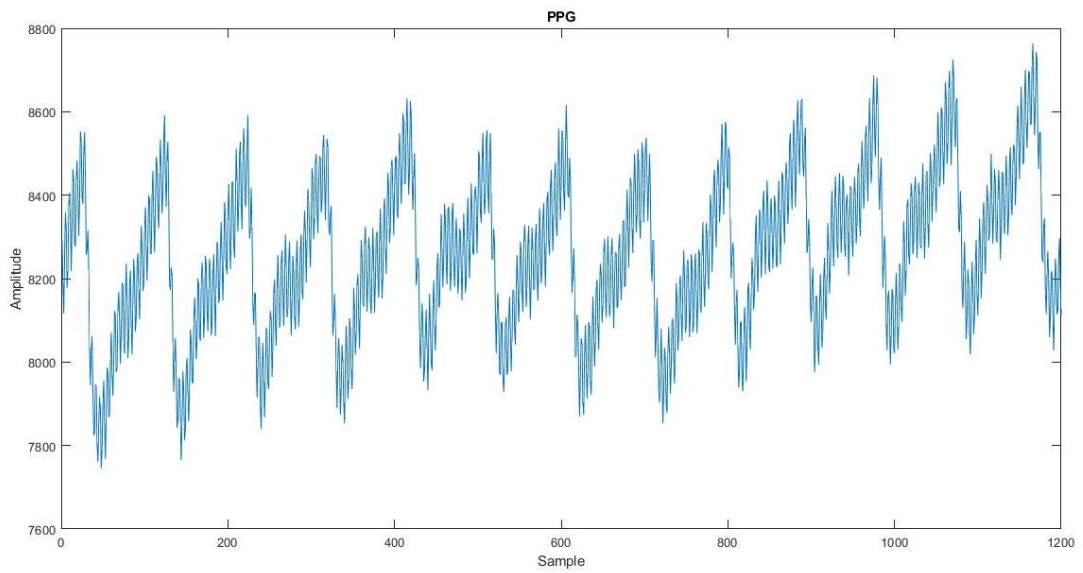


Figure 36: Figure 37: Raw data of PPG signal - acquisition 3

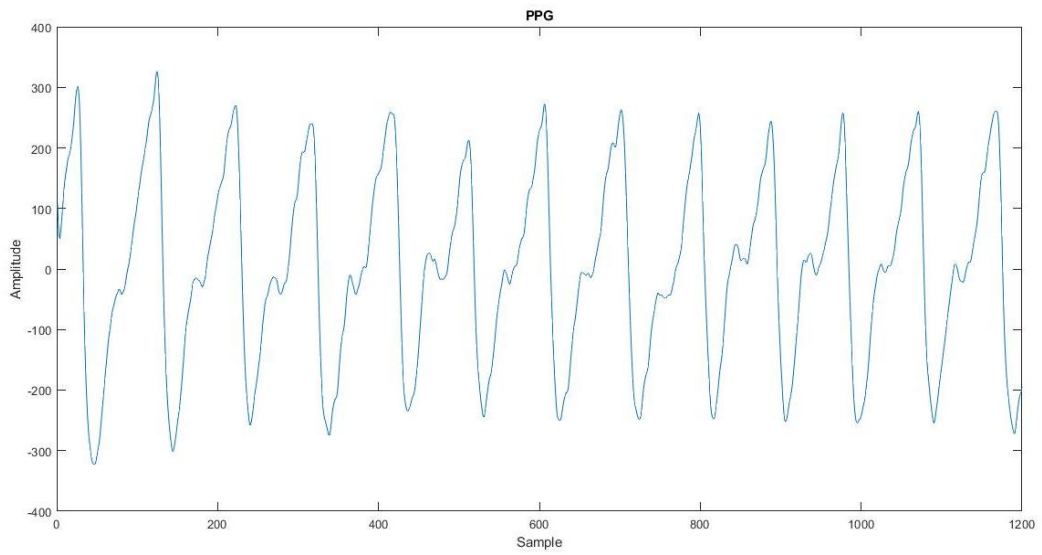


Figure 38: Filter PPG signal - acquisition 3

13. Discussion

The design of the prototype is well-define. Every sensor is connected to the developing board and communicates data to the client without looseness.

The Bluetooth module allows to transmit in real-time a lot of data. This is one of the fundamental parameters for a wearable sensor, that does not include an internal storage system, capable to conserve data for a long time.

The outcomes of ECG sensors look promising. The waveform of ECG is comparable with a traditional electrocardiogram.

The sensor *Max30001* shows high accuracy to extract physiological data, as it can be observed from the ECGs signal coming from the simulator. *Max30001* is one of the most used integrated sensors for wearable cardiac monitoring devices and the result of this work confirms its potential as a monitor of cardiac activity.

The raw data of real people appear noisy, due to many significant factors The electrodes were positioned on the cute without a traditional gel patch, provoking random and no predictable relative movements between the cute and the electrodes. Moreover, other sources of disturbance are respiration and motion artefact. No filter is set on the hardware, even if the *Max30001* allows the implementation of a high or a low pass filter at different frequencies. The client receives raw data to evaluate the integrity and sensitivity of the sensor.

Nevertheless, the noise to signal ratio is always higher than 0.

Two Butterworth filters are implemented and applied to the signal during signal processing analysis.

The processed signals are comparable with traditional ECG tacks; the characteristic points are clearly visible. The calculated Heart Rate is in the physiological range (60-90 bpm).

In the second trial of experiments, the prototype also includes a third electrode, the Body Bias electrode. The datasheet of Max3001 indicates this configuration. Adding the Body Bias electrode improves the quality of the signal, which results in less sensitivity than the signal acquired by two exploiting electrodes. Thus, the Body Bias will be integrated into the final device.

As it could be predicted, the signal is corrupted by the non-voluntary movement of the subject. The implementation of a low-pass filter reduces the effect of the artefact of movement. In any case, the outcomes of this study show that the ECG signal can be extracted even if the raw data are corrupted by a high quantity of noise.

Considering the outcomes of PPG acquisitions, the configuration with one green LED does not appear suitable for furthermore applications. Wearable devices are commonly used to track and control biomedical parameters, estimated from raw PPG data, which requires at least two emitters at different wavelengths. For example, optical sensors based on the match of LEDs and photodiodes are the standard technologies of the commercial oximeter.

Nevertheless, the single LED was used to collect PPG waveform from finger and wrist to define settings for the acquisition, like sampling frequency, filter cut-off frequency.

Conclusion

Wearable devices could become a very potent tool for long-term continuous monitoring during the routine daily lives of individuals. The improvement in technologies of the small integrated system and wireless communication is the root of the spread of this new portable, cheap, and comfortable device.

They would also show a significant potential of reducing health care costs by preventing unnecessary hospitalizations as well as enabling better self-management and intervention approaches.

Concerning this work, the first acquisitions with this new multiparametric device look promising. Especially, the tested ECG sensor results are suitable for the wearable application, because the device can detect bioelectrical signals even if in presence of significant disturbances.

The future experimental trial of the device will concern the PPG sensors with multiwavelength LEDs. This kind of optical sensor, accomplished with the algorithm of signal processing and physiological parameters extraction, is used in many wearable devices for fitness tracks. It could also become a potential instrument to monitor biological signals, thank the improvements in optical signal knowledge.

In the future, this device could be implemented to be wear and used during daily activity and to follow up patients after their hospitalization period.

Bibliography

- [1] C. L. Stanfield, *Principle of Human Physiology*, Alabama: Pearson, 2013.
- [2] J. M. Pevnick, K. Birkeland, R. Zimmer, Y. Elad e I. Kedan, «Wearable technology for cardiology: an update and framework for the future,» *Trends in cardiovascular medicine* , vol. 28.2, pp. 144-150, 2018.
- [3] F. Sana, M. E. Isselbacher, J. P. Singh, E. Heist, B. Pathik e A. A. Armoundas, «Wearable Devices for Ambulatory Cardiac Monitoring: JACC State-of-the-Art Review.,» *J Am Coll Cardiol*, vol. 7, n. 75(13), pp. 1582-1592, 2020.
- [4] P. M. Barrett, R. Komatireddy, S. Haaser, S. Topol, J. Sheard, J. Encinas, A. J. Fought e E. J. Topol, «Comparison of 24-hour Holter Monitoring with 14-day Novel Adhesive Patch Electrocardiographic Monitoring.,» *The American Journal of Medicine*, vol. 127, n. 1, pp. 95.11-95.17, 2014.
- [5] D. Castaneda, A. Esparza, M. Ghamari, C. Soltanpur e H. Nazeran, «A review on wearable photoplethysmography sensors and their potential future applications in health care,» *International Journal of Biosensors & Bioelectronics*, vol. 4(4), p. 195, 2018.
- [6] P. P. Banik, S. Hossain, T.-H. Kwon e H. Kim, «Banik, P. P., Hossain, S., Kwon, T. H., Kim, H., & Kim, K. D. Development of a wearable reflection-type pulse oximeter system to acquire clean PPG signals and measure pulse rate and SpO2 with and without finger motion.,» *Electronics*, vol. 9(11), p. 1905, 2020.
- [7] S. Hossain, T.-H. Kwon e K.-D. Kim, «Comparison of different wavelengths for estimating SpO2 using beer-lambert law and photon diffusion in PPG,» *IEEE International Conference on Information and Communication Technology Convergence (ICTC)*, pp. 1377-1379, 2019.
- [8] T. Tamura, Y. Maeda, M. Sekine e M. Yoshida, «Wearable Photoplethysmographic Sensors—Past and Present,» *electronics*, vol. 3, pp. 282-302, 2014.
- [9] R. Anderson e E. Parris, « The optics of human skin,» *Dermatol*, vol. 77, pp. 13-19, 1981.
- [10] M. Kramer, A. Lobbestael, E. Barten, J. Eian e G. Rausch, «Wearable Pulse Oximetry Measurements on the Torso, Arms, and Legs: A Proof of Concept,» *Military Medicine* , vol. 182 (3/4), p. 92, 2017.

- [11] J. Allen, «Photoplethysmography and its application in clinical physiological measurement,» *Physiological measurement*, vol. 28, n. 3, p. R1, 2007.
- [12] L. Hooseok, K. Hoon e L. Jinseok, «Reflectance pulse oximetry: Practical issues and limitations,» *Ict Express*, vol. 2(4), pp. 195-198, 2016.
- [13] K. Li e S. Warren, «A wireless reflectance pulse oximeter with digital baseline control for unfiltered photoplethysmograms,» *IEEE transactions on biomedical circuits and systems*, vol. 4(4), pp. 269-278, 2012.
- [14] S. K. Longmore, G. Y. Lui, G. Naik, P. P. Breen e B. Jalaludin, «A comparison of reflective photoplethysmography for detection of heart rate, blood oxygen saturation, and respiration rate at various anatomical locations,» *Sensors*, vol. 19, n. 8, p. 1874, 2019.
- [15] N. Meir, R. Ayal e K. Robert, «Pulse oximetry: fundamentals and technology update,» *Medical Devices: Evidence and Research*, vol. 7, p. 231, 2014.
- [16] M. Nitzan, S. Noach, E. Tobal, Y. Adar, Y. Miller, E. Shalom e S. Engelberg, «Calibration-Free Pulse Oximetry Based on Two Wavelengths in the Infrared — A Preliminary Study,» *sensors*, vol. 14, pp. 7420-7434, 2014.
- [17] T. Sondej, K. Rózanowski e D. Sondej, «Reflectance Method for a Wearable Photoplethysmographic Sensor—Experimental Evaluation,» *The Polish Journal of Aviation Medicine*, vol. 22(1), p. 5, 2016.
- [18] R. Stojanovic e D. Karadagic, «Design of an Oximeter Based on LED-LED Configuration and FPGA Technology,» *Sensors*, vol. 13, pp. 574-586, 2013.
- [19] W. Verkruyssen, M. Bartula, E. Bresch, M. Rocque, M. Meftah e I. Kirenko, «Calibration of Contactless Pulse Oximetry,» *Anesthesia and analgesia*, vol. 124 (1), p. 136, 2017.
- [20] C. Wei, L. Sheng, G. Lihua, C. Yuquan e P. Min, «Study on conditioning and feature extraction algorithm of photoplethysmography signal for physiological parameters detection,» *4th International Congress on Image and Signal Processing, IEEE*, vol. 4, pp. 2194-2197, 2011.
- [21] Q. Zhang, D. Arney, J. M. Goldman e E. M. Isselbacher, «Design Implementation and Evaluation of a Mobile Continuous Blood Oxygen Saturation Monitoring System,» *sensors*, vol. 20(22), p. 6581, 2020.
- [22] F. P. Branca, *Fondamenti di Ingegneria Clinica*, Italia: Springer Verlag, 2000.